Nader A. Naderi

Candidate

Electrical & Computer Engineering

Department

This thesis is approved, and it is acceptable in quality and form for publication on microfilm:

Approved by the Thesis Committee:

, Chairperson

Accepted:

Dean, Graduate School

Date

QUANTUM DOT GAIN-LEVER LASER DIODE

BY

NADER A. NADERI

B.S., APPL. PHYSICS, MASHHAD UNIVERSITY, 2000

THESIS

Submitted in Partial Fulfillment of the
Requirements for the Degree of

Master of Science
Electrical Engineering

The University of New Mexico
Albuquerque, New Mexico

December, 2007

ACKNOWLEDGMENTS

I would like to thank my advisor and thesis committee chairman, Professor Luke F. Lester for all of his support and expert guidance which helped me to find my path and learn a lot on semiconductor lasers through these years.

In addition, special thanks are due to my thesis committee members Professor Sanjay Krishna and Professor Christos G. Christodoulou who gave me great help and insightful comments in completing this thesis. I also gratefully thank my committee chair and members for reviewing my thesis and providing valuable comments and suggestions.

I wish to acknowledge my gratitude to Dr. Anthony Martinez for helping me on using the high-speed laser characterization measurement setup. I would also like to thank Prof. Vassilios Kovanis, Yan Li, Dr. Yongchun Xin and Christopher Dziak for their helpful advice and assistance during this research.

Finally, I would like to thank my wife Shadi, for her endless support and understanding through these years. To my dad for all of his encouragement and finally to my mom despite that she is not between us, her love will be always in my heart.

This investigation was supported in part by US. Army and Air force Research Laboratories, at Center for High Technology Materials (CHTM), University of New Mexico.

QUANTUM DOT GAIN-LEVER LASER DIODE

BY

NADER A. NADERI

ABSTRACT OF THESIS

Submitted in Partial Fulfillment of the
Requirements for the Degree of

Master of Science
Electrical Engineering

The University of New Mexico
Albuquerque, New Mexico

December, 2007

Quantum Dot Gain-Lever Laser Diode

by

Nader A. Naderi

B.S., Applied Physics, Mashhad University, 2000

M.S., Electrical Engineering, University of New Mexico, 2007

Abstract

Semiconductor quantum dot (QD) lasers are competitive candidates for many applications such as high-speed long-haul optical communication systems. This is due to their superior lasing characteristics (compared to conventional quantum well (QW) lasers and also their potential for high differential gain and direct modulation with negligible chirp. Recently, substantial efforts have been made to improve the modulation characteristics of QD semiconductor lasers such as enhancing the modulation efficiency and improving the overall modulation bandwidth.

The gain lever effect is a method used to enhance the efficiency of amplitude modulation and optical frequency modulation at microwave frequencies by taking advantage of the sub-linear nature of the gain versus carrier density.

Previously, two-section quantum well lasers have been investigated theoretically and experimentally to explore the gain lever effect. As for QD devices, which are extremely promising because of the strong gain saturation effect in dots, have not been investigated until recently.

In this thesis, first the characteristics and applications of conventional two-section gain lever semiconductor lasers are presented. In related previous studies, gain levered single and multiple QW lasers have been used to enhance the modulation efficiencies in both intensity (IM) and frequency (FM) modulation. In this work, the modulation characteristics of a gain lever QD laser diode is demonstrated for the first time.

In this work we report an amplitude modulation enhancement of 8-dB for a p-doped two-section quantum dot laser and discuss the relation between the normalized 3-dB bandwidth and the modulation section gain for different power levels.

Also based on rate equations and small signal analysis, a novel modulation response equation is derived to describe the device dynamics. Using the new modulation response function the actual gain lever ratio can be measured for various power levels.

For future work, the gain lever laser structure can be optimized to reduce the effect of non-linear gain suppression which directly limits the efficiency enhancement through the damping factors and relaxation oscillation frequency.

TABLE OF CONTENTS

LIST OF FIGURES x

Chapter 1 1

INTRODUCTION TO QUANTUM DOT LASERS 1

1.1 A Brief History 1

1.2 Advantages of Quantum Dots over Quantum Wells 2

1.3 High-Speed Modulation of Semiconductor Lasers 6

1.4 The Gain-Lever Effect 7

1.5 Thesis Objectives 8

1.6 Chapter 1 References 10

Chapter 2 14

MODULATION DYNAMICS OF SEMICONDUCTOR LASERS 14

2.1 Introduction 14

2.2 Rate Equations-Basic Theory 15

2.3 Small-Signal Analysis 21

2.4 Modulation Response Function 23

2.5 Modulation Bandwidth 26

2.6 Non-Linear Mechanisms in Semiconductor Lasers 29

2.6.1 Non-Linear Gain Saturation 30

2.6.2 Carrier Transport 33

2.7 Chapter 2 References 36

Chapter 3 ..... **39**

THE GAIN-LEVER EFFECT IN SEMICONDUCTOR LASERS **39**

3.1 Introduction 39

3.2 The Gain-Lever Effect in Quantum Well Lasers 40

3.3 Previous Gain-Lever Formulations for Intensity Modulation 43

3.4 Chapter 3 References 50

Chapter 4 ..... **52**

QUANTUM DOT GAIN-LEVER LASER DIODE **52**

4.1 Motivation for the QD Gain-Lever Laser 52

4.1.1 Gain Saturation in Quantum Dots 54

4.2 Experimental Results 56

4.2.1 Device Structure 56

4.2.2 Device Characteristics and QD Gain Model 58

4.2.3 Modulation Characteristics 62

4.2.4 Experimental Setup 64

4.2.5 Modulation Efficiency Enhancement 65

4.2.6 3-dB Modulation Bandwidth 68

4.2.7 Modulation Response Function for Single-Section Lasers 71

4.3 Novel Two-Section Modulation Response Model 74

4.4 Summary and Conclusion 85

4.5 Chapter 4 References 88

LIST OF FIGURES

Figure (1.1) *Density of states function for Bulk, Quantum Well, Quantum Wire, and Quantum Dot structure*……..…….……..…….3

Figure (2.1) *Steady-state dependence of the lasing power on the injection current and lasing spectrum for a 1.3μm p-doped QD laser*…….……..……...20

Figure (2.2) *Simulation of the relative modulation response function of a semiconductor laser for different photon densities*……...……..…….25

Figure (2.3) *Uniform damping rate as a function of resonance frequency squared for an ideal laser diode*…….……..28

Figure (3.1) *Schematic diagram of a two-contact single QW laser and the gain versus carrier density plot*…….……..……41

Figure (3.2) *Modulation responses for different pumping levels applied to the modulation section*……..……47

Figure (4.1) *A comparison of the variation of the material gains in Quantum Dot and Quantum Well as a function of carrier density*……...…….55

Figure (4.2) *Schematic layer diagram of the 10-stack InAs/InGaAs DWELL laser structure under the investigation..*……..…..…….……..57

Figure (4.3) *P-I curve and lasing spectrum of the two-section QD device under investigation and the differential quantum efficiency as a function of cavity length, curve-fitted with equation (4.2)...*……..……...…….. 59

Figure (4.4) *Threshold gain as a function of threshold current density at room temperature*……...……...61

Figure (4.5) *Schematic diagram of a two-section quantum dot laser with gain versus carrier density curve showing bias points for both sections and schematic view of the experimental setup*……..……...63

Figure (4.6) *Modulation responses for uniform and asymmetric pumping cases in the two-section QD laser*……..…….67

Figure (4.7) *Normalized 3-dB bandwidth as a function of gain in the modulation section*……..……70

Figure (4.8) *Normalized resonance frequency as a function of gain in the modulation section plotted based on the single-section model.*……...……72

Figure (4.9) *Damping rate under uniform pumping case as a function of resonance frequency squared*……..……..……..……...……76

Figure (4.10) *Measured modulation response for the asymmetric pumping case* ($G_{a0} / G_{th} = 0.5$) *curve-fitted with one and two-section modulation response models*……..……..……..……81

Figure (4.11) *Normalized resonance frequency as a function of normalized gain in the modulation section plotted based on the new two-section model, and extracted damping rates associated with the modulation and the gain section plotted as a function of normalized modulation section gain*……..……..……..……...83

Chapter 1

INTRODUCTION TO QUANTUM DOT LASERS

1.1 A Brief History

The performance of semiconductor lasers developed dramatically after the invention of double hetrostructure lasers (DHL) in which both carrier and optical mode confinement [1, 2, 3, 4 and 5] improvements resulted in reduction of the threshold current density and also enabled continuous wave operation at room temperature[6, 7]. Further developments were achieved by using quantum well (QW) structures in which the carriers are confined within quantized energy levels due to the reduction in the physical space volume in one dimension [8, 9, 10 and 11]. This structure helps to reduce the threshold and allows for some control over the wavelength by changing the thickness of the well.

After the success of the QW hetrostructure, demonstration of quantum-dot (QD) lasers was one of the most important steps in the field of semiconductor lasers [12, 13 and 14]. A quantum dot is a semiconductor crystal whose size is on the order of a few nanometers to a few tens of nanometers. The quantum dot, which typically consists of a small bandgap semiconductor embedded in a larger bandgap material, confines electrons, holes,

or electron-hole pairs to zero dimensions in a region on the order of the electrons' de Broglie wavelength.

This confinement in all directions leads to discrete quantized energy levels that can be controlled by changing the size and shape of the QDs. Due to the delta-function-like density of states in QDs, devices fabricated from these novel materials provide many superior characteristics such as ultralow threshold current [15], small linewidth enhancement factor, and low temperature dependence of the threshold current [16].

1.2 Advantages of Quantum Dots over Quantum Wells

Advantages of QDs compared with QWs are due to their unique density of states resulting from three-dimensional confinement of carriers. The main idea of making a zero-dimensional quantum confined structure was developed by changing the quantum structure from one to three dimensions, initially called "multi-dimensional quantum well" [17]. This change in the dimensional structure can be realized by comparing the change in the density of states of bulk, quantum well, quantum wire and quantum dot, which respectively have zero, one, two and three-dimensional carrier confinement. As shown in figure (1.1), bulk materials have a continuous density of states that is also proportional to the square root of energy. In QWs, the step-function-like density of states decreases compared to the bulk material. In quantum wires, the density of states decreases compared to the QWs and finally the density of states in QDs is a δ-function in energy.

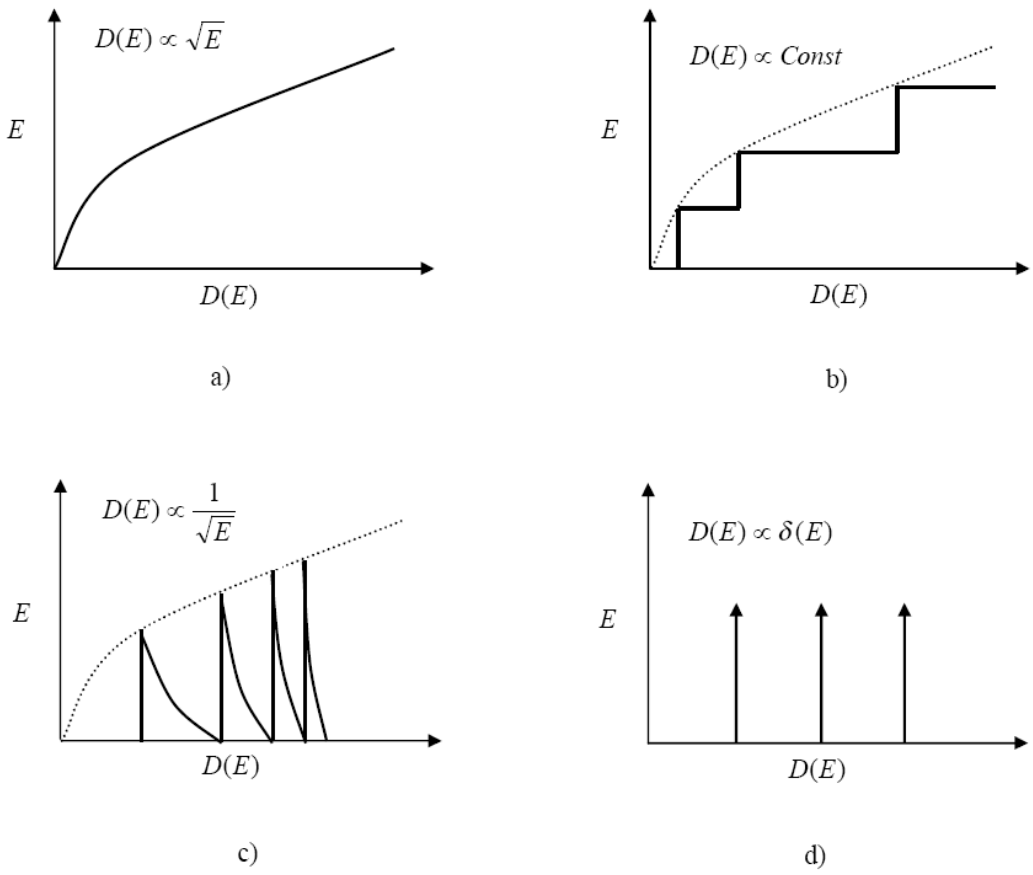

Figure (1.1) *Density of states function for (a) Bulk, (b) Quantum Well, (c) Quantum Wire, and (d) Quantum Dot structure*

Because of these atom-like discrete levels and a δ-function density of states, QDs are expected to have many useful properties for optoelectronic applications compared to quantum well and double hetrostructure lasers:

Ultra-Low threshold current density

It has been predicted that the threshold current density of QD lasers should be lower than that of QW lasers due to the reduction in the density of states in dots [18]. This is because in QDs due to the smaller active material, there are fewer carriers necessary to invert the electronic states resulting in extremely low threshold current densities. So far the lowest threshold current density reported for 1.3 μm quantum dot lasers are in the range of 17 to 42 A/cm^2 [15, 18] with the lowest at 10 A/cm^2 under pulsed pump which was demonstrated by our research group.

High characteristic temperature T_0 (Low temperature dependence of threshold current density)

In very small QDs, the spacing between the atomic-like states is greater than the available thermal energy, so thermal depopulation of the lowest electronic states is inhibited. Therefore in properly-designed QD lasers, the threshold current is not as sensitive to temperature [18]. The threshold current dependence of the temperature can be described by characteristic temperature, T_0, since it has been empirically determined that there is an exponential relation between threshold current density and temperature

as $I_{th} = I_0 e^{(\frac{T}{T_0})}$. High T_0 values reported for QDs correspond to less variation of threshold current density with temperature, which is desirable in semiconductor lasers.

Small linewidth enhancement factor

The linewidth enhancement factor, α, is an important dynamic figure of merit for applications such as high-speed fiber optic communications. The linewidth enhancement factor is defined as the ratio of change in the real part of the index of refraction as a function of carrier density to the change of the imaginary part of index of refraction as a function of carrier density. The δ-function-like density of states in QD materials can be modeled as a Gaussian function, which leads to symmetric optical gain spectrum. Using the Kramers-Kronig relation between the real and imaginary (gain) parts of the index of refraction yields a zero linewidth enhancement factor at the peak gain location in QDs. The linewidth enhancement factor is also inversely proportional to the differential gain, and it is evident that large differential gains are attainable in QD lasers. Therefore, low α-factors can be expected and value of 0.1 has been reported in conventional QD lasers [19].

High-frequency modulation

As described before, quantum dots have a δ-function-like density of states, which results in both high material gain and high differential gain. These two factors

theoretically contribute to a high modulation bandwidth [20]. However, some factors such as slow carrier relaxation time and smaller optical gain (longer photon lifetime) can limit the modulation bandwidth of QD lasers.

1.3 High-Speed Modulation of Semiconductor Lasers

Semiconductor lasers have become one of the most important elements in fiber optic links due to their superior modulation characteristics, size and cost efficiency. The typical laser wavelengths in coherent light communication systems based on semiconductor lasers are 1.3 μm and 1.55 μm, which correspond to the minimum dispersion and attenuation wavelengths, respectively. The device's operating or carrier frequency is around 200 THz and its signal can be modulated directly or externally either in RF (Radio Frequency) varying from 10 KHz to 300 MHz or microwave frequency (300MHz-30 GHz).

Direct modulation, involves changing the current input around the bias level above threshold. It is principally a simpler method and is easier to implement rather than the external modulation, but the output light produced depends on internal dynamics of the laser. Therefore, in order to improve the modulation characteristics such as obtaining higher modulation bandwidth or enhanced modulation efficiency we need to be able to control some of the intrinsic laser parameters such as optical gain or optical confinement factor.

There have been many efforts made to improve direct modulation of semiconductor lasers. This challenge actually began with the invention of new materials such as QWs and QDs with better carrier and photon confinement that led to higher gain and differential gain and gradually improved by developing better waveguiding and current injections structures. Meanwhile other modulation techniques have been used to improve the modulation characteristics. For instance direct modulation based on modulation of the optical confinement factor used to enhance the modulation bandwidth in single QW structures [22].

In the following chapter the theory of direct modulation in semiconductor lasers and related modulation parameters are discussed in detail by using the rate equation analysis, and the conventional modulation response model of a single section laser for both ideal and realistic cases is described.

1.4 The Gain-Lever Effect

Nowadays there is an increasing interest to use high-speed optical communication systems to transmit digital and analog signals through optical fiber links. Optical fiber links are desirable for these applications since they are cheap, light, and immune to electromagnetic interference.

Directly modulated semiconductor lasers are the most efficient candidates for high-speed communication in microwave frequencies since they are compact and have

relatively low cost of fabrication. One possible method to improve the modulation characteristics of semiconductor lasers is through the technique of the optical gain-lever in a two-section laser diode. This method is based on the sub-linear relationship between the optical gain and the carrier density (approximated in this thesis by the dependence of gain with injected current density), and previously has been studied to enhance the efficiency of direct intensity modulation (IM) and optical frequency modulation (FM) of a two-section QW laser [23, 24, 25]. The modulation efficiency is increased by RF modulating only one of the sections, which is DC-biased such that the differential gain is substantially higher than the case of the single-section laser. A detailed theory behind this effect and its impact on the modulation characteristics of semiconductor lasers will be discussed in the following chapters.

1.5 Thesis Objectives

As described in the first section of this chapter, QDs have many potentially superior characteristics such as high material and differential gain, and the potential for superior direct modulation capability. These factors are essentially required in order to improve the high-speed modulation characteristics. Therefore lasers fabricated from these novel materials can be considered as a serious candidate for ultra-high speed applications.

Enhancing the high-speed modulation of quantum dot lasers by taking advantage of the gain-lever effect is studied for the first time in this thesis.

In chapter 2, the basic theory related to modulation of the semiconductor lasers is described, and related issues and limitations in this field are discussed. Chapter 3 goes through the gain-lever basic theory and the impact of this effect on high-speed modulation characteristics. In the same chapter the previous research related to using the gain-lever effect on QW devices for various applications is summarized. In chapter 4, the experimental data is presented and a novel modulation response model is derived for a two-section configuration. As will be seen in the same chapter, the new response model can be considered as a proper replacement for the single-section modulation response model that was previously used in QW gain-lever devices. Finally the QD results will be compared to those from previous work on gain-levered QW devices including modulation efficiency enhancement, 3-dB bandwidth, and limitations due to non-linear gain. Also the possible solutions that can improve the high-speed characteristics using the gain-lever effect in QDs will be presented.

1.6 Chapter 1 References

[1] Zh. I. Alferov, V. M. Andreev, E. L. Portnoi, M. K. Trukan, "AlAs-GaAs heterojunction injection lasers with a low room-temperature threshold," *Sov. Phys. Semicond.,* 3, 1107-1110, (1970) and H. Kroemer, "A proposed class of heterojunction injection lasers," *Proc. IEEE*, 51, 1782–1784, (1963)

[2] Zh. I. Alferov, V. M. Andreev, D. Z. Garbuzov, Yu. V. Zhilyaev, E. P. Morozov, E. L. Portnoi, and V. G. Trofim, "Effect of heterostructure parameters on the laser threshold current and the realization of continuous generation at room temperature," *Sov. Phys. Semicond.,* 4, 1573-1575, (1970)

[3] I. Hayashi, M. B. Panish, P. W. Foy and S. Sumski, " Junction lasers which operate continuously at room temperature," *Appl. Phys. Lett.,* 17, 109-111, (1970)

[4] R. D. Dupuis, and P. D. Dapkus, "Very low threshold $Ga_{1-x}Al_xAs$-GaAs double-heterostructure lasers grown by metalorganic chemical vapor deposition," *Appl. Phys. Lett.,* 32, 473-475, (1978)

[5] C. Gmachl, F. Capasso, D. L. Sivco, and A. Y. Cho, "Recent Progress In Quantum Cascade Lasers And Applications," *Reports On Progress In Phys.,* 64 1533-1601, (2001)

[6] Z. I. Alferov, V. M. Andreev, V. I. Korol'kov, E. L. Portnoi, and D.N. Tret'yakov, "Injection properties of n-Al Ga As-p-GaAs hetero-junctions," *Fiz. Tekh. Poluprovodn.,* 2, 1016 1017, (1968), *Sov.Phys. Semicond.,* 2, 843-844, (1969)

[7] I. Hayashi, M. B. Panish, P. W. Foy, and S. Sumski, "Junction lasers which operate

continuously at room temperature," *Appl. Phys. Lett.,* 17, 109-111, (1970)

[8] R. D. Dupuis, P. D. Dapkus, N. Holonyak Jr., E. A. Rezek, R. Chin, "Room Temperature operation of quantum-well $Ga_{1-x}Al_xAs$-GaAs laser diodes grown by metalorganic chemical vapor deposition," *Appl. Phys. Lett.,* 32, 295-297, (1978)

[9] W. T. Tsang, "Extremely low threshold (AlGa)As modified multiquantum well heterostructure lasers grown by molecular-beam epitaxy," *Appl. Phys. Lett.,* 39, 786-788, (1981)

[10] W. T. Tsang, "Extremely low threshold (AlGa)As graded-index waveguide separate-confinement heterostructure lasers grown by molecular-beam epitaxy," *Appl. Phys. Lett.,* 40, 217-219, (1982)

[11] N. Chand, E. E. Becker, J. P. Van der Zeil, S. N. G. Chu, and N. K. Dutta, "Excellent uniformity and very low (less-than-50A/cm2) threshold current density strained InGaAs quantum-well diode-lasers on GaAs substrate," *Appl. Phys. Lett.,* 58, 1704-1706, (1991)

[12] J. L. Pan, "Intraband Auger Processes And Simple Models Of The Ionization Balance In Semiconductor Quantum-Dot Lasers," *Physical Review B-Condensed Matter,* 49, 11272-11287 (1994)

[13] N. N. Ledentsov, V. M. Ustinov, A. Yu. Egorov, *et al.*, "Optical properties of heterostructures with InGaAs–GaAs quantum clusters," *Phys. Semicond.,* 28, 832, (1994)

[14] N. Kirstaedter, N. N. Ledentsov, M. Grundmann, *et al.*, "Low threshold, large T_o injection laser emission from (InGa)As quantum dots," *Electron. Lett.,* 30, 1416, (1994)

[15] A. Stintz, G. T. Liu, H. Li, L. F. Lester, and K. J. Malloy, "Low Threshold Current Density 1.3μm InAs quantum dot lasers with the Dots-in-a-Well (DWELL) structure," *IEEE Photon. Technol. Lett.,* 13, (2000)

[16] H. Y. Liu, T. J. Badcock, K. M. Groom, M. Hopkinson, *et al*, "High-performance 1.3-μm InAs/GaAs quantum-dot lasers with low threshold current and negative characteristic temperature," *Proc. SPIE Int. Soc. Opt. Eng.,* France (2006)

[17] Y. Arakawa, and H. Sakaki, "Multidimensional quantum well laser and temperature dependence of its threshold current," *Appl. Phys Lett.,* 40 (11), 939-941, (1982)

[18] G. Park, O. B. Shchekin, D. L. Huffaker, D. G. Deppe "Low-Threshold Oxide-confined 1.3 μm Quantum-Dot Laser," *IEEE Photon. Technol. Lett.,* 13, 230-232, (2000)

[19] T. C. Newell, D. Bossert, A. Stintz, B. Fuchs, K. J. Malloy, and L. F. Lester, "Gain And Linewidth Enhancement Factor In InAs Quantum Dot Laser Diodes," *IEEE Photon. Technol. Lett.,* 11, 1527, (1999)

[20] K. Y Lau and A. Yariv, "Ultrahigh Speed Semiconductor Lasers," *IEEE J. Quantum Electron.,* 21, 121-138, (1985)

[21] A. Frommer, S. Luryi, D. T. Nichols, J. Lopata, and W. S. Hobson, "Direct modulation and optical confinement factor modulation of semiconductor lasers," *Appl. Phys. Lett.,* 67, 1645-1647, (1995)

[22] D. Gajic and K. Y. Lau, "Intensity noise in the ultrahigh efficiency tandem-contact QW lasers," *Appl. Phys. Lett.,* 57, 1837-1839, (1990)

[23] N. Moore and K. Y. Lau, "Ultrahigh efficiency microwave signal transmission using

tandem-contact single QW GaAlAs lasers," *Appl. Phys. Lett.,* 55, 936-938, (1989)

[24] K. Y. Lau, "Gain-levered semiconductor laser-direct modulation with enhanced frequency modulation and suppressed intensity modulation," *IEEE Photon. Technol. Lett.,* **3**, 703-705, (1990)

Chapter 2

MODULATION DYNAMICS OF SEMICONDUCTOR LASERS

2.1 Introduction

There has been much research devoted to realizing the basic physics describing the high-speed modulation of semiconductor lasers. High-frequency direct-modulated lasers are in large demand for applications such as high-speed optical communications, phased array radars, microwave optical fiber links, cable TV and many more due to their superior modulation characteristics and low cost.

In order to understand the basic physics and improve the direct modulation of semiconductor lasers, it is necessary to choose the right tools to predict the physical behavior of the device under the modulation and then find the limiting factors and explore the best way to mitigate them. High-speed dynamics of semiconductor lasers have been conventionally modeled using a set of two coupled first-order linear differential equations. In this chapter the ideal rate equations and their solutions under small-signal direct amplitude (analog) modulation will be reviewed. More realistic cases will be discussed later on this chapter when some factors due to the non-linear effects are introduced in the traditional rate equations. To conclude the limiting factors, these non-linear phenomena will be summarized.

2.2 Rate Equations-Basic Theory

One of the most important aspects of laser operation is its transient behavior. When the drive current applied to the device is modulated, it is desired to see how the laser responds to this modulation and whether the output light reproduces the driven current pulse or not. As a matter of fact, this behavior also determines the modulation bandwidth of the device. To understand this transient behavior some mathematical tools called rate equations are necessary to track the net fluctuations of both carriers and photons, which are supplied by injected current and stimulated emission, respectively. In order to derive these rate equations, some initial assumptions need to be considered. First it is assumed that the active region has low impurity concentration and therefore the injected carrier density is equal to the electron or hole concentration in the band. Also, due to the small dimension of the laser it is assumed that carrier and photon densities along the propagation direction are constant and only a single lasing mode is presented in the cavity [1]. Using the assumptions mentioned above and considering various physical phenomena through which the electron concentration, N, changes with time inside the active region, the net rate of change of N, in three dimensions is defined as [2]:

$$\frac{dN}{dt} = \frac{I}{eV} - \frac{N}{\tau_{sp}} - GP \qquad (2.1)$$

where I is the injection current, V is the volume of the optical gain medium, τ_{sp} is the carrier recombination lifetime (or spontaneous carrier lifetime) which includes the loss of the electrons due to both spontaneous emission and nonradiative recombination, G is

the unclamped material gain in which the group velocity, v_g, is implicit ($v_gG \rightarrow G$) and P is the photon density. In the right-hand side of the equation, I/eV corresponds to carrier injection, N/τ_{sp} is the carrier loss via spontaneous emission and GP represent the carrier-photon interaction and also corresponds to the loss via stimulated emission.

To understand how carriers interact with photons, a second rate equation is required for photons, which are significantly supplied through stimulated emission and to some extent by spontaneous emission coupled into the lasing mode.

It is also important to note that τ_{sp}, depends on the carrier density N, (due to the Auger recombination, bimolecular radiative recombination and Shockley-Read-Hall recombination) and decreases with carrier density as N^2 for QWs and bulk semiconductors. By considering the fact that photons are actually depleted through cavity losses, the net rate of change of the photon density can be written as [2]:

$$\frac{dP}{dt} = \Gamma GP - \frac{P}{\tau_p} + \frac{\beta N}{\tau_{sp}} \qquad (2.2)$$

where in this equation P again is the photon density, Γ is optical confinement factor (~0.1), τ_p (~1-10 ps) is the photon lifetime in the cavity and β represent the fraction of spontaneous emission that couples into the laser cavity mode. The terms on the right-hand side of this equation represent the rate of increase due to the stimulated photon emission, loss due to cavity and coupling losses, and spontaneous emission rate into the mode respectively. The photon lifetime, τ_p, is considered as the average time that the photon remains in the cavity before it gets absorbed or emitted through the facets and is

related to the cavity loss (combination of internal loss plus mirror losses) as [3]:

$$\frac{1}{\tau_p} = v_g(\alpha_i + \alpha_m) = v_g \alpha_{cav} \qquad (2.3)$$

After analyzing the dynamic performance of the laser in terms of the rate equations, it is important to look at the steady-state case to understand the static characteristics. In the steady-state situation, the device has already been through the initial transient effects and there will be no more fluctuation in the carrier and photon density with time. Therefore the time derivatives in the left-hand side of equations (2.1) and (2.2) are equal to zero. Also the factor, β, the spontaneous emission factor, is usually very small (order of 10^{-4}) and can be neglected. Therefore the last term in equation (2.2) will vanish. Then the steady-state rate equation gives the relation describing the gain and optical loss balance as:

$$\Gamma G_0 = G_{th} = (\alpha_i + \alpha_m) \qquad (2.4)$$

where G_{th} is the total modal gain at threshold and G_0 is the gain at threshold. This equation indicates that, when lasing action occurs, the threshold current I_{th} compensates for all the carrier losses and for any injection current above threshold, the carrier density remains at the threshold density value N_{th}. However a slight increase might occur due to the gain compression or by carrier non-uniformity [4] which will be discussed later in this chapter. Typical threshold current values are in the 5-50 mA range for a high-speed laser diode, depending on the size of the active volume and fundamental laser structure.

From the steady-state rate equations, the DC or steady-state coherent photon density P_0 can be obtained as:

$$P_0 = \eta_S (I - I_{th}) = \eta_i \tau_p \frac{(I - I_{th})}{eV} \qquad (2.5)$$

and the threshold current is defined as:

$$I_{th} = \frac{N_{th} eV}{\tau_{sp}} \qquad (2.6)$$

where in equation (2.5), η_S [W/A] is the slope efficiency which is related to the differential quantum efficiency η_d (probability that an electron injected above threshold contributes a photon to the coherent laser beam) and depends on the cavity length. It is usually desired to achieve high slope efficiency and for that the internal losses of electrons and photons need to be minimized. Carrier leakage can be reduced by having a good lateral and vertical carrier confinement in the active region and photon absorption can be reduced by less doping of optical confinement layers and smoother waveguides. Lower mirror reflectivity and cavity length can improve the slope efficiency but at the expense of a higher threshold current density. η_i is the internal quantum efficiency that represents the fraction of the total current increase above the threshold which results in stimulated emission of photons [5].

Since the DC carrier density remains constant above the threshold and the stimulated lifetime is shorter than the spontaneous lifetime, the internal quantum efficiency, η_i, limits out on the injection efficiency, η_{inj}, which is typically 0.8 or higher for QD lasers.

Finally, the total output power emitted through both facets can be written as:

$$Power_{(output)} = v_g \alpha_m h\nu P_0 V \qquad (2.7)$$

Equation (2.5) gives the common expression for the *P-I* curve above the threshold, where the emission properties of a semiconductor laser and its related parameters can be easily characterized. Figure (2.1) shows the *P-I* curve of a 1.3 μm QD laser with 1.5 mm cavity length operating at 20 °C. As illustrated in this figure, the *P-I* curve can tell us what is the threshold current of the device and also shows the current necessary to obtain a certain amount of power. At room temperature, the threshold current is about 35 mA and the laser can emit over 1.2 mW of output power from each facet at 45 mA of applied current.

The laser performance depends on the temperature of operation and it degrades at high temperatures which is a practical problem for many high-speed lasers in the field. As mentioned in previous chapter, this temperature sensitivity is found to increase the threshold current density exponentially as:

$$I_{th} = I_0 \exp(\frac{T}{T_0}) \qquad (2.7.1)$$

where I_0, is a constant and T_0 is the characteristic temperature that is used to express the temperature sensitivity of threshold current.

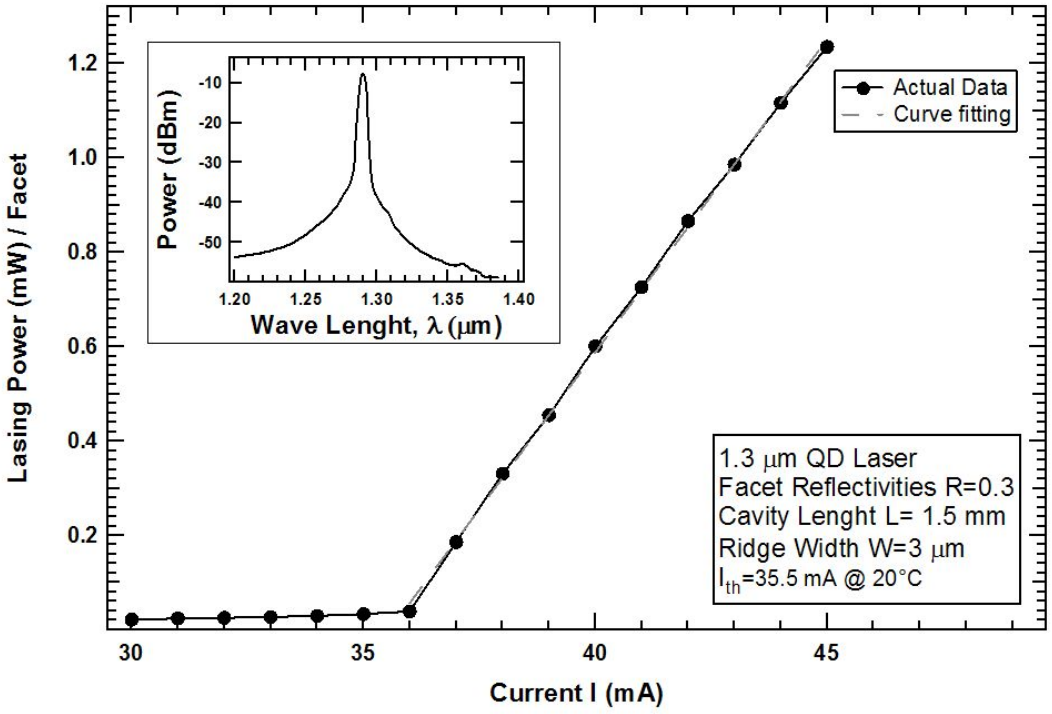

Figure (2.1) *Steady-state dependence of the lasing power on the injection current (P-I curve) and lasing spectrum for a 1.3 μm p-doped QD laser*

So far, we have reviewed the fundamental equations describing the basic steady-state characteristics of the laser. In following section we will discuss the small-signal analysis, in order to linearize the rate equations and solve them analytically for an ideal case.

2.3 Small-Signal Analysis

In analog modulation, sinusoidal current variations will be added to the initial steady-state injection current. The modulation response of semiconductor lasers is studied by solving the rate equations introduced before with a time-varying current as [3]:

$$I(t) = I_0 + i_m f_p(t) \qquad (2.8)$$

where I_0 is the steady-state input current, i_m is the modulation current and f_p is the shape of the current pulse. In the case of small-signal analysis it is possible to obtain the analytic solutions for these rate equations. In this analysis the laser is biased above the threshold such that applied current I_0 is greater than I_{th} and is modulated such that the variation in modulation current is much smaller than the difference between the applied and threshold current ($i_m << I_0$-I_{th}) that leads to the variation of N, and P which are much smaller than the steady-state values N_{th}, P_0 respectively. Therefore it is possible to linearize the rate equations and solve them analytically [5], by using the Fourier-transform technique for an arbitrary shape of the current pulse $f_p\ (t)$. In this linearization the spontaneous carrier lifetime, τ_{sp}, and the linear gain coefficient G' representing the differential gain, are introduced.

In analog modulation, the steady-state input DC current, I_0, is superimposed with a small ac signal and in a simple case of only one angular frequency ω and constant amplitude i_m, the injection current in equation (2.8) becomes:

$$I(t) = I_0 + i_m e^{j\omega t} \qquad (2.9)$$

Similar to the injection current, and by using the complex frequency domain notation, the carrier and photon densities can be also expressed as the sum of their steady-state value plus a small ac component:

$$N = N_0 + n_m e^{j\omega t} \qquad (2.10)$$

$$P = P_0 + p_m e^{j\omega t} \qquad (2.11)$$

By substituting equations (2.9) through (2.11) into the original rate equations (2.1) and (2.2) and considering the terms that are first order in ω, the following relationships are obtained:

$$j\omega n_m = \frac{i_m}{eV} - (\frac{1}{\tau_{sp}} + G'P_0)n_m - G_0 p_m \qquad (2.12)$$

$$j\omega p_m = \Gamma G' n_m P_0 + (G_{th} - \frac{1}{\tau_p}) p_m \qquad (2.13)$$

where $G'=dG/dN$ is the linear gain coefficient also known as the differential gain in which the group velocity is implicit ($v_g dG/dN \rightarrow dG/dN$) and as is defined before $G_0=G(N_{th})$ is the material gain at threshold . As mentioned above, under the steady-state condition there will be no change in the rate of photon and carrier densities with time and therefore the left-hand side of equations (2.1) and (2.2) will be equal to zero.

Under steady-state condition the photon lifetime relation with the threshold gain is defined as $\frac{1}{\tau_p} \equiv G_{th}$, which theoretically shows that the photon lifetime will remain constant at threshold (again for simplicity $v_g G_{th} \rightarrow G_{th}$). Using the photon lifetime expression in equation (2.13), the second term in this equation will be zero and (2.13) reduces to:

$$j\omega p_m = \Gamma G' n_m P_0 \qquad (2.14)$$

Now from the small-signal solutions to the rate equations we can simply derive the high-speed modulation response function for semiconductor lasers.

2.4 Modulation Response Function

By using equations (2.12), (2.14) and considering the small signal response of the photon density with the change in current, the expression for the relative modulation response is derived as:

$$R(\omega) = \frac{p_m(\omega)/i_m(\omega)}{p_m(0)/i_m(0)} = \frac{\omega_0^{\,2}}{(\omega_r^{\,2} - \omega^2) + j\omega\gamma} \qquad (2.15)$$

where ω_r is the angular frequency at which the response function peaks for low photon densities and is called the angular resonance frequency or relaxation oscillation frequency and γ is the damping factor. The modulation response is flat (R (ω) =1) for frequencies such that $\omega << \omega_r$, and peaks at $\omega = \omega_r$ and drops rapidly for $\omega >> \omega_r$. Simply the angular

resonance frequency and the damping factor can be described as:

$$\omega_r = 2\pi f_r = \sqrt{\frac{G'P_0}{\tau_p}} = \sqrt{G_{th}G'P_0} \qquad (2.16)$$

$$\gamma = \omega_r^{\,2}\tau_p + \frac{1}{\tau_{sp}} \qquad (2.17)$$

It is important to note that the damping factor detunes the resonance peak of the response. As a result, the relaxation oscillation frequency is not necessarily always considered to be the same as the peak frequency.

This response characteristic reaches a maximum at the peak frequency ω_{peak} which is slightly smaller than the resonance frequency ω_r. The peak frequency can easily be found by taking the derivative of the response function equation (2.15), with respect to ω and setting it equal to zero. Then the resultant peak frequency, ω_{peak}, is defined as:

$$\omega_{peak} = \sqrt{\frac{2\omega_r^{\,2} - \gamma^2}{2}} \qquad (2.18)$$

As seen in the expression above, under low photon densities, γ^2 is much smaller than $2\omega_r^2$, and therefore the peak frequency can be approximated by the resonance frequency in this case.

The absolute modulation response function $\left|R(\omega = 2\pi f)\right|^2$ can be also found from equation (2.15) and expressed as a function of *"f"* as follows:

$$\left|R(f)\right|^2 = \frac{f_r^{\,2}}{\left[(f_r^{\,2} - f^2)^2 + (\frac{\gamma}{2\pi})^2 f^2\right]} \qquad (2.19)$$

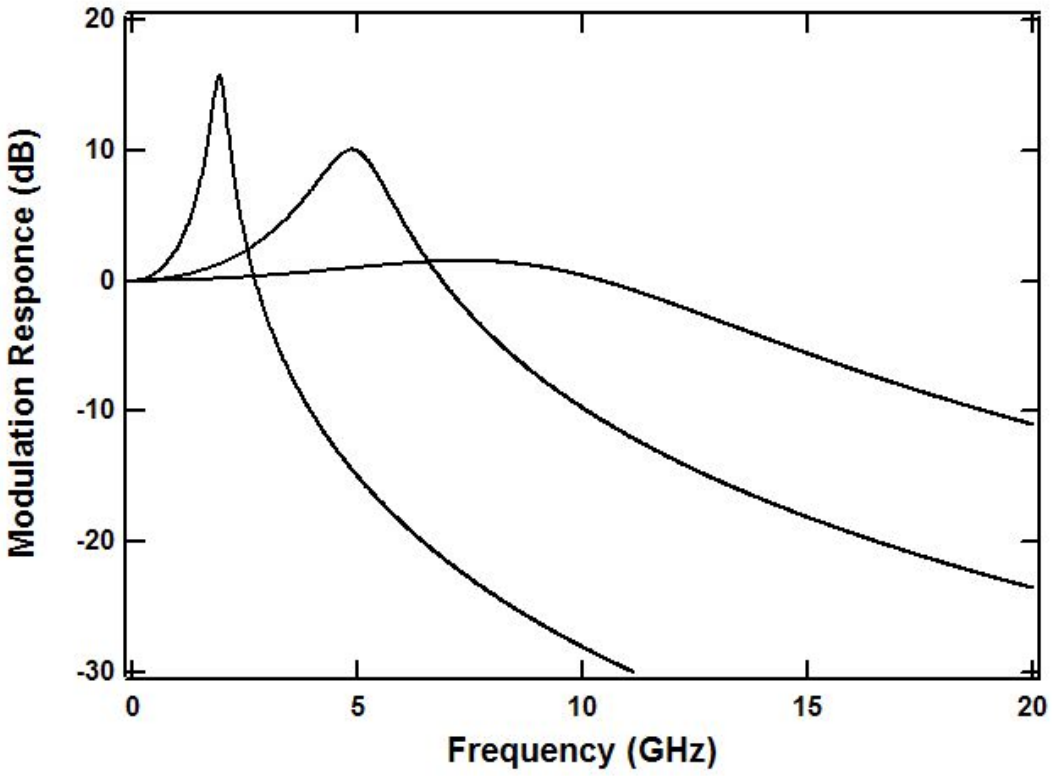

Figure (2.2) *Simulation of the relative modulation response function of a semiconductor laser for different photon densities*

The response function expressed in equation (2.19) is plotted as function of frequency for various photon densities in figure (2.2). As shown in this figure, for higher photon densities, the resonance frequency f_r and damping rate, γ, increase and as a result the response becomes flatter. Therefore the damping term indicated in the response function is considered as one of the most important limiting factors in the modulation of semiconductor lasers.

2.5 Modulation Bandwidth

The 3-dB modulation bandwidth, f_{3dB}, is defined as the frequency at which the output signal drops to $\left|R(2\pi f_{3dB})\right| = 2^{-\frac{1}{2}} =$ -3 dB. So in order to obtain the 3-dB bandwidth we need to set $\left|R(\omega = 2\pi f)\right|^2 = \frac{1}{2}$ and solve for $\omega=2\pi f$ which will give us:

$$\omega_{3dB}{}^2 = \omega_r{}^2 - \frac{\gamma^2}{2} + \sqrt{\left(\omega_r{}^2 - \frac{\gamma^2}{2}\right)^2 + \omega_r{}^4} \qquad (2.20)$$

With low damping and low injection current where $\omega_r{}^2 >> \frac{1}{2}\gamma^2$ equation (2.20) reduces to a simpler expression as:

$$\omega_{3dB} \cong 1.55\omega_r \qquad (2.21)$$

The maximum bandwidth of directly modulated lasers can be limited due to several reasons. At high injection current the bandwidth reaches a maximum value due to

increased damping, device heating, gain compression, carrier transport or parasitic RC effects [6]. We will briefly discuss a couple of these limiting factors and their effect on the modulation bandwidth later in this chapter.

It is convenient to express the 3-dB bandwidth in terms of frequency, f, rather than angular frequency, ω. Also the relationship between the resonance frequency, f_r, and the damping factor, γ, defines the *K-factor* as:

$$\gamma = \frac{1}{\tau_{sp}} + Kf_r^2 \qquad (2.22)$$

The *K-factor* can be calculated from the slope of γ as a function of resonance frequency squared, f_r^2, as shown in figure (2.3). The range of damping factor, γ, and an estimated carrier recombination lifetime, τ_{sp}, can be found from the intersection of the curve with the y-axis in this figure.

Usually, a lower value of *K-factor* is desired (It is typically on the order of several nanoseconds), but this factor is also known as a figure of merit in high-speed modulation of semiconductor lasers since it depends on the resonance frequency and damping rate. At high photon densities or high optical powers, it is possible to neglect the effect of $1/\tau_{sp}$. This assumption reduces equation (2.22) to:

$$\gamma = Kf_r^2 \qquad (2.23)$$

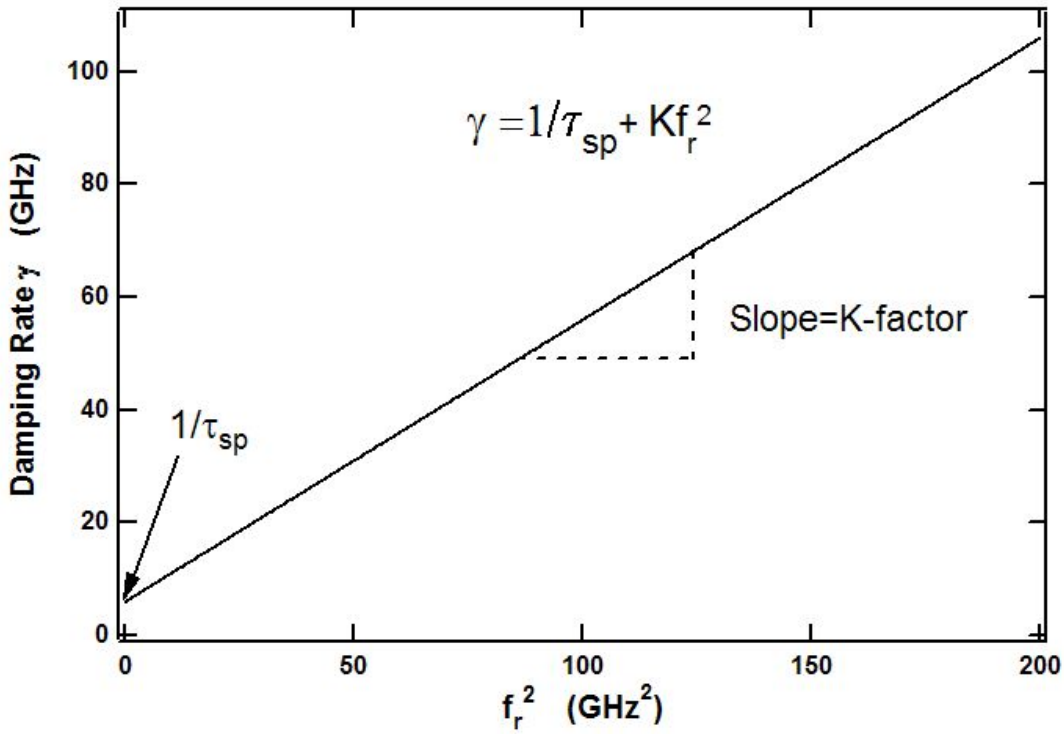

Figure (2.3) *Uniform damping rate as a function of resonance frequency squared for an ideal laser diode*

Using the expression in (2.23), we can define the 3-dB bandwidth of equation (2.20) as:

$$f^2{}_{3dB} = f_r^2 - \frac{K^2 f_r^4}{8\pi^2} + \sqrt{\left(f_r^2 - \frac{K^2 f_r^4}{8\pi^2} \right)^2 + f_r^4} \qquad (2.24)$$

For most cases it is possible to assume that $4\pi^2 f_r^2 \tau_p >> \frac{1}{\tau_{sp}}$, so the damping factor can be approximated as $\gamma \cong 4\pi^2 f_r^2$ and we can derive the maximum 3-dB bandwidth by taking the derivative of equation (2.24) and setting it equal to zero.

Equation (2.24) is maxima when $f_r^2 = \frac{8\pi^2}{K^2}$ and therefore the maximum 3-dB bandwidth can simply be defined as:

$$f_{3dB-\max} = \frac{2\pi\sqrt{2}}{K} \approx \frac{8.89}{K} \qquad (2.25)$$

In the following section we will review some non-linear mechanisms that limit the modulation bandwidth in semiconductor lasers.

2.6 Non-Linear Mechanisms in Semiconductor Lasers

So far, we have considered the ideal case for direct modulation and neglected many realistic phenomena that directly affect the high-speed modulation characteristics of semiconductor lasers. These effects, including non-linear gain saturation and carrier transport, can significantly affect the maximum achievable bandwidth of the device and overall laser performance. Although there are many phenomena that may affect the

modulation performance of the device, two of the most fundamental mechanisms that can directly limit the modulation bandwidth and high-speed performance of the device will be reviewed.

2.6.1 Non-Linear Gain Saturation

Non-linear gain saturation with photon density is one of the fundamental non-linear effects through which the observation of additional damping in the resonance peak can be explained.

The linear gain approximation as $G=G'(N-N_0)$ was previously used in the ideal small-signal analysis. In reality the optical gain is reduced at higher photon densities [7] and the physical mechanism behind this reduction can be explained by various phenomena such as spatial hole burning, spectral hole burning, carrier heating and two photon absorption [8, 9, 10, 11, 12 and 13]. For instance, as mentioned above at high photon density, the optical gain reduces due to a depletion of electron-hole pairs. This spectral hole burning (SHB), within the energy distribution of carriers restricts further stimulated recombination [9].

In order to take the effect of non-linear gain saturation into the account we need to introduce a non-linear gain parameter (or gain compression factor), ε, into the gain function as:

$$G \rightarrow \frac{G}{1+\varepsilon P} \qquad (2.26)$$

A typical value of the non-linear gain parameter ε is on the order of 10^{-17} cm^3 for bulk

materials. Now by introducing the non-linear gain saturation concept to the initial rate equations, (2.1), and (2.2) change to:

$$\frac{dN}{dt} = \frac{I}{eV} - \frac{N}{\tau_{sp}} - \frac{GP}{1+\varepsilon P} \qquad (2.27)$$

$$\frac{dP}{dt} = \frac{\Gamma GP}{1+\varepsilon P} - \frac{P}{\tau_p} + \frac{\beta N}{\tau_{sp}} \qquad (2.28)$$

where the linear gain is replaced by the non-linear gain expression, using equation (2.26) and other parameters remain the same. Using equations (2.9) through (2.11) for small signal analysis and keeping terms with first order in ω, new expressions can be obtained as:

$$j\omega n_m = \frac{i_m}{eV} - (\frac{1}{\tau_{sp}} + \frac{G'P_0}{1+\varepsilon P_0})n_m + G_0\left(\frac{P_0\varepsilon}{(1+\varepsilon P_0)^2} - \frac{1}{1+\varepsilon P_0}\right)p_m \qquad (2.29)$$

Again and for simplicity, the differential gain is defined as $G' = \frac{dG}{dN}$ and $G_0=G\ (N_{th})$ is the material gain at threshold.

The photon lifetime expression changes to:

$$v_g(\alpha_i + \alpha_m) = \frac{1}{\tau_p} = \frac{G_{th}}{1+\varepsilon P_0} \qquad (2.30)$$

In the photon density rate equation if we substitute for the inverse photon lifetime using equation (2.30) and apply the non-linear gain saturation concept to it, we will have:

$$j\omega p_m = \frac{\Gamma G'P_0}{1+\varepsilon P_0} n_m - \frac{P_0 G_{th}\varepsilon}{(1+\varepsilon P_0)^2} p_m \qquad (2.31)$$

Using the equations (2.29), through (2.31) we can derive the expression for the modulation response function as:

$$R(\omega) = \frac{s_m(\omega)}{i_m(\omega)} = \frac{A}{\omega_r^{\,2} - \omega^2 + j\omega\gamma} \qquad (2.32)$$

where $A = \dfrac{\Gamma G' P_0}{eV(1+\varepsilon P_0)}$. Similarly, the resonance frequency and damping factor change to the following:

$$\omega_r = \sqrt{\frac{G' P_0}{\tau_p (1+\varepsilon P_0)}\left(1 + \frac{\varepsilon}{G'\tau_{sp}}\right)} \qquad (2.33)$$

As mentioned before, the non-linear gain coefficient, ε, is a number on the order of 10^{-17} cm^3. So in equation (2.33) the second term in parenthesis can be neglected compared to 1 and the resonance frequency expression reduces to:

$$\omega_r = \sqrt{\frac{G' P_0}{\tau_p (1+\varepsilon P_0)}} \qquad (2.34)$$

And the damping factor can be defined as:

$$\gamma = \omega_r^{\,2}\left(\frac{\varepsilon}{G'} + \tau_p\right) + \frac{1}{\tau_{sp}} \qquad (2.35)$$

Again the damping rate can be expressed as a function of carrier lifetime and *K-factor* as $\gamma = K f_r^{\,2} + \dfrac{1}{\tau_{sp}}$, where $K = 4\pi^2\left(\tau_p + \dfrac{\varepsilon}{G'}\right)$.

As seen in equation (2.34), the resonance frequency is significantly affected by the non-linear gain saturation phenomena and reduces with the square root of $(1+\varepsilon P_0)$.

Also the non-linear gain effect has a strong impact on the *K-factor* making it the principal limiting factor for the maximum 3-dB bandwidth in high-speed modulation. This impact can be better observed in QD lasers due to the strong gain compression in these devices [14].

2.6.2 Carrier Transport

Carrier transport (including diffusion, tunneling) in QW lasers has a significant effect on the modulation properties of high-speed lasers (i.e. damping rate) via a reduction of the effective differential gain and usually is a significant limit [15]. Therefore in order to obtain a more accurate model it is necessary to include this effect, as well as non-linear gain saturation in the fundamental equations, derived so far.

In this case, an additional damping rate exists due to the process of capture and escape of the carriers into and from the QW respectively. Thereby, the damping factor does not necessarily vary linearly with photon density. This model changes the traditional rate equations by introducing different carrier densities in the barrier and the well. Also the transport factor $\chi = (1+\tau_{esc}/\tau_c)$ which depends on laser structure, is introduced to this model in order to emphasize the effect of carrier transport time, τ_c (including diffusion to and capture into the QW) and escape time, τ_{esc}. In this model, by introducing the carrier transport effect and considering the non-linear gain saturation we can obtain a better modulation response function that gives a more realistic result compared to that of the

ideal case. The resultant modulation response function can be expressed as [15]:

$$R(\omega) = \frac{s_m(\omega)}{i_m(\omega)} = \left(\frac{1}{1 + j\omega\tau_c} \right) \frac{A}{\omega_r^{\,2} - \omega^2 + j\omega\gamma} \qquad (2.36)$$

where $A = \dfrac{\Gamma \dfrac{G'}{\chi} P_0}{eV(1 + \varepsilon P_0)}$.

As seen in equation (2.36), the response function is affected by an additional term (low pass filter) which introduces a low frequency roll-off to the modulation response and can be considered as a serious limitation to the maximum possible bandwidth.

The resonance frequency and damping factor also can be expressed as follows:

$$f_r = \sqrt{\frac{\dfrac{G'}{\chi} P_0}{4\pi^2 \tau_p (1 + \varepsilon P_0)}} \qquad (2.37)$$

$$\gamma = K f_r^{\,2} + \frac{1}{\tau_{sp}} \qquad (2.38)$$

where $K = 4\pi^2 \left(\tau_p + \dfrac{\chi\varepsilon}{G'} \right)$ and τ_{sp} is the spontaneous emission carrier lifetime [16].

As indicated in the expression above, depending on the laser structure, the *K-factor* can be significantly affected by carrier transport, since the non-linear gain factor, ε, weakly depends on the laser structure [15]. Larger values of transport factor, χ, leads to a decrease in the effective differential gain and therefore decreases the resonance frequency.

Finally this model gives rise to the following expression for optical modulation response as a function of frequency:

$$|R(f)|^2 = \frac{f_r^{\,2}}{\left[(f_r^{\,2} - f^2)^2 + (\frac{\gamma}{2\pi})^2 f^2\right]\left[1 + (2\pi f \tau_c)^2\right]} \qquad (2.39)$$

This model and the response function extracted from is used to predict and study the damping behavior in high-speed, single-section semiconductor lasers.

Some useful techniques such as optimizing the device structure can be used to decrease the delays introduced by carrier transport and to some extent decrease the non-linear gain compression in direct modulation lasers.

Other than optimizing the intrinsic device parameters, some other techniques have been used to improve the high-speed modulation of semiconductor lasers. In the following chapter, we will review the optical gain-lever mechanism in direct modulation of semiconductor lasers, which previously has been used to enhance the modulation efficiency and performance of QW lasers [17, 18, and 19].

Then the QD gain-lever laser diode will be introduced which is demonstrated for the first time in this thesis and the relative advantages and limitations of using this mechanism in QDs will be discussed.

2.7 Chapter 2 References

[1] P. Bhattacharya, "Semiconductor Optoelectronics Devices," 2nd edition, *Prentice-Hall,* Ch. 7, 317-325 (1997)

[2] K. Y. Lau, N. Bar-Chaim, I. Ury, Ch. Harder, and A. Yariv, "Direct modulation of short-cavity GaAs lasers up to X-band frequencies," *Appl. Phys. Lett.,* 43, 1 (1983)

[3] G. P. Agrawal, "Fiber-Optic Communication Systems," 3rd edition, *John Wiley & sons, Inc.,* Ch. 3, 106-112 (2002)

[4] J. Piprerek, P. Abraham, and J. E. Bowers, "Carrier non uniformity effect on the internal efficiency of the multi-quantum well laser diodes," *Appl. Phys. Lett.,* 74 (4), 489-91, (1999)

[5] L. A. Coldren and S. W. Corzine, "Diode lasers and photonic integrated circuits," *John Wiley & Sons,* (1995)

[6] K. L. Lear, A. Mar, K. D. Choquette, S. P. Kilcoyne, R. P. Schneider, and K. M. Geib, "High-frequency modulation of oxide-confined vertical-cavity surface emitting lasers," *Electron. Lett*., **32**, 457–8, (1996)

[7] K. Y. Lau, "gain-levered semiconductor laser-direct modulation with enhanced frequency modulation and suppressed intensity modulation," *IEEE Photon. Technol. Lett.,* 3, 703-705, (1991)

[8] G. P. Agrawal, "Gain nonlinearities in semiconductor lasers: Theory and application to distributed feedback lasers," *IEEE J. Quantum Electron.,* 23, 860 (1987)

[9] G. P. Agrawal, "Effect of gain and index nonlinearities on single-mode dynamics in

semiconductor lasers," *IEEE J. Quantum Electron.,* 26, 1901 (1990)

[10] G. P. Agrawal and G. R. Gray, "Importance of Nonlinear gain in semiconductor lasers," *Proc. SPIE,* 1497, 444 (1991)

[11] C. Z. Ning and J. V. Moloney, "Plasma-heating induced intensity-dependent gain in semiconductor lasers," *Appl. Phys. Lett.,* 66, 559 (1995)

[12] J. E. Bowers, "High speed semiconductor laser design and performance," *Solid-State Electron.,* 30, 1 (1987)

[13] D. J. Channin, "Effect of gain saturation on injection laser switching," *J Appl. Phys.,* 50, 3858 (1979)

[14] H. Su, L. F. Lester "Dynamic Properties of QD DFB Lasers: high speed, linewidth and chirp," *J. Appl. Phys.* 38, 2112-2118, (2005)

[15] R. Nagarajan, M. Ishikawa, T. Fukushima, R. S. Geels and J. E. Bowers, "High speed QW lasers and carrier transport effect," *IEEE J. Quantum Electron.,* 28, 1990-2007, (1992)

[16] P. Bhattacharya, D. Klotzkin, O. Qasaimeh, W. Zhou, S. Krishna, and D. Zhu, "High-speed Modulation and Switching Charactristics of InGaAs-AlGaAs Self-Organized QD Lasers," *IEEE J. Selected Topics in Quantum Electron.,* 6, 426-438, (2000)

[17] K. J. Vahala, M. A. Newkirik, and T. R. Chen, "The optical gain-lever: a novel gain mechanism in the direct modulation of QW semiconductor lasers," *Appl. Phys. Lett.,* 54, 25, (1989)

[18] N. Moore and K. Y. Lau, “Ultrahigh efficiency microwave signal transmission using tandem-contact single quantum well GaAlAs lasers,” *Appl. Phys. Lett*., 55, 936 (1989)

[19] W. M. Yee and K. A. Shore, “Enhanced wavelength tenability in asymmetric gain-levered QW semiconductor laser,” *IEEE J. Lightwave Technol.,* 13, 4 (1995)

Chapter 3

THE GAIN-LEVER EFFECT IN SEMICONDUCTOR LASERS

3.1 Introduction

In Chapter 1, we briefly talked about the gain-lever effect and its impact on various applications such as direct amplitude and optical frequency modulation in semiconductor lasers [1, 2]. Previously several approaches have been proposed to increase the modulation efficiency of semiconductor lasers using the gain-lever modulation. In this chapter we will summarize the previous work on direct amplitude modulation of QW lasers, based on the optical gain-lever technique and possible approaches to enhance this effect.

The optical gain-lever was first realized by K. J. Vahala, *et al.* in 1989 by demonstrating the enhancement of the amplitude modulation produced by either optical or electrical modulation of QW lasers [3]. Before that, the idea of producing parasitic-free modulation in semiconductor lasers was developed using a technique called "active layer photo-mixing" by the same group in 1988 [4, 5, 6]. In this method, the light produced by two single-mode laser sources was mixed and optically pumped the active layer of another laser diode, producing a carrier density modulation. The dynamic modulation response extracted from this optical gain technique was observed to cover a reasonable range of

frequencies. It was then suggested that a two-segment configuration in a laser diode could be used to produce a net gain in the conventional carrier modulation of semiconductor lasers. This technique became known as the "gain-lever effect" [3].

3.2 The Gain-Lever Effect in Quantum Well Lasers

The physical origin of the gain-lever effect can be explained by the concept of optical gain saturation with carrier density in semiconductors. As mentioned in chapter 1, the change in different dimensional structures can be realized by comparing the change in the density of states of bulk, quantum well, quantum wire and quantum dot media, which respectively have zero, one, two and three-dimensional carrier confinement. The optical gain increases by injecting excess carriers and is directly related to the density of states function. As a result the available optical gain is not equal for different structures. For instance, bulk materials have a continuous density of states that is also proportional to the square root of energy, but in QWs, the density of states increases as a step-function-like compared to the bulk material. Therefore optical gain vs. carrier density in QWs first increases rapidly and then saturates faster than in bulk materials and as a result, the differential gain in QWs also changes more with gain compared to bulk materials. By knowing the gain vs. carrier density behavior, the basic concept of the gain-lever effect in semiconductor lasers can be theoretically realized.

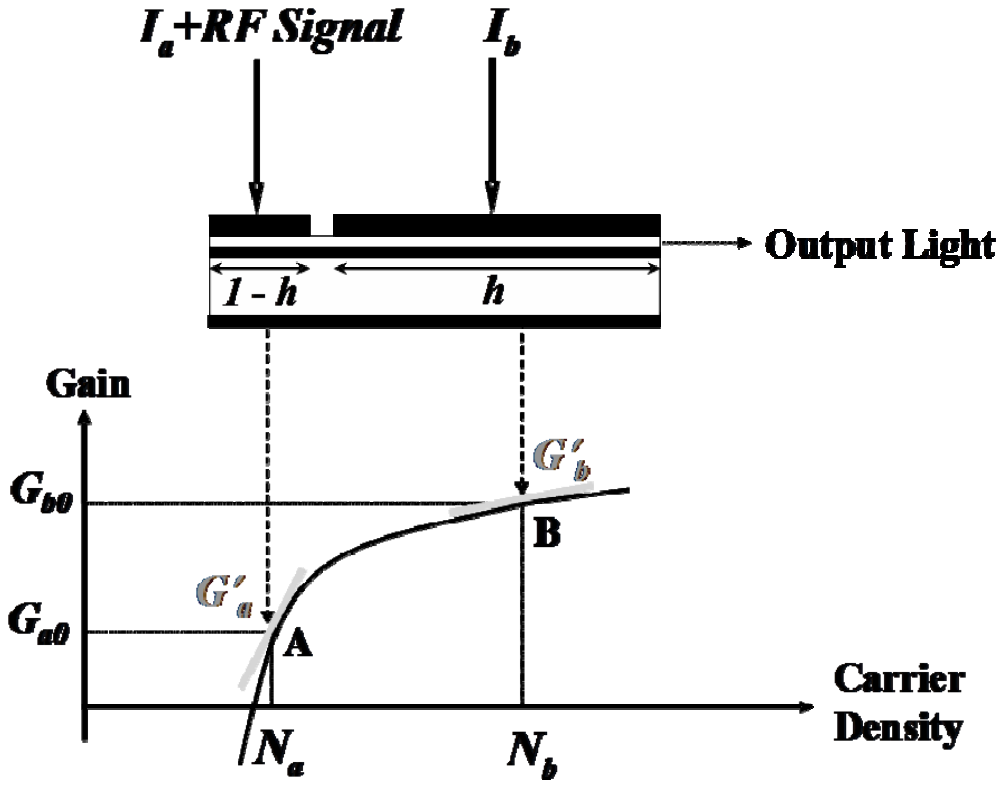

Figure (3.1) *Schematic diagram of a two-contact single QW laser and the gain versus carrier density [7]*

The idea of the gain-lever effect was further elucidated in 1989 by N. Moore and K. Y. Lau [7]. They introduced the first gain-lever laser structure based on a two-section, single QW laser having two anode contacts and a single cathode (The two anode configuration is sometimes called a tandem contact). Figure (3.1) shows the schematic view of the device with a typical gain versus carrier density characteristic of a single QW laser.

In this configuration, section (a), corresponds to the shorter or modulation section where the ac signal is applied and the longer section (b) or gain section is DC biased in order to perform the most of amplification. Finally *h* is the fractional length of the gain section. In order to run the device as a gain-lever, the gain section (section b) is biased at high gain and the modulation section (section a) is biased at low gain level as seen in the diagram. When the operation point of the device is chosen well above threshold, (steady-state operation) the overall modal gain is firmly clamped to the threshold value which cannot be exceeded even with strongly increased pump powers. At this point the gain is exactly clamped to the value of the optical cavity losses (if we neglect the small energy coupled to the lasing mode from spontaneous emission). Therefore as shown in figure (3.1), since the total gain is clamped above the threshold and due to the non-linear dependence of gain with carrier density, any small change in carrier density in the modulation section (corresponds to high differential gain regime) as a result of injection current variation, produces a much larger variation in carrier density in the gain section (corresponds to low differential gain regime) and consequently in the total number of photons.

In another words, one can obtain a large change in the carrier density in the gain section by applying a small change in injection current in the modulation section. In such a case an RF optical gain will result when the differential gain in the modulation section, G'_a, is greater than the differential gain in the gain section, G'_b. This is the point at which the desired gain-lever effect occurs.

Since 1989, much research work based on the gain-lever effect has been conducted to achieve very high efficiencies in intensity (IM) and frequency (FM) modulation [3, 7, 8, and 9].

3.3 Previous Gain-Lever Formulations for Intensity Modulation

In this section, the theoretical formulations of the gain-lever effect in direct intensity modulation of a single QW laser will be reviewed. This theory was provided by Lau for the first time [7]. In order to understand the physics of the gain-lever and characterize the resultant intensity modulation based on this effect, a set of new rate equations was suggested and linearized by small-signal analysis.

Since the reservoir of photons is readily exchanged between the gain and modulation sections, the photon density rate equation is adopted from the conventional model and rearranged based on the gain-lever device parameters as [7]:

$$\frac{dP}{dt} = \left\{ \Gamma P[G_a(1-h) + G_b h] - \frac{P}{\tau_p} \right\} \qquad (3.1)$$

where P is the photon density, τ_p, is the photon lifetime, Γ is the optical confinement factor and G_a, G_b, are the unclamped gain in the modulation and gain sections, respectively. As seen in equation (3.1) the total optical gain is equal to the sum of the related section gain multiplied by its corresponding fractional length. Since each section is biased at a different current level, the rate of change in carrier density will not be equal in the two-sections, thereby two different rate equation need to be introduced corresponding to each section [7]:

$$\frac{dN_a}{dt} = \frac{J_a}{ed} - BN_a^{\,2} - G_a P \qquad (3.2.1)$$

$$\frac{dN_b}{dt} = \frac{J_b}{ed} - BN_b^{\,2} - G_b P \qquad (3.2.2)$$

where N_a, N_b, are the carrier densities in sections *a, b,* and J_a, J_b, are the corresponding current densities in sections *a, b.* The carrier density square dependence corresponds to the band-to-band bimolecular recombination form used for QW structures where B is the bimolecular recombination constant.

Using the small-signal approximation, the solution to these rate equations was derived as [7]:

$$\frac{p}{j_a} = \frac{\Gamma G'_{a0} P_0 (1-h)(s+\gamma_b)/ed}{s^3 + (\gamma_a + \gamma_b)s^2 + A_1 s + A_2} \qquad (3.3)$$

where,

$$A_1 = \Gamma P_0 \left[G_{a0} G'_{a0} (1-h) + G_{b0} G'_{b0} h \right] + \gamma_a \gamma_b , \qquad (3.3.1)$$

$$A_2 = \Gamma P_0 \left[G_{a0} G'_{a0} \gamma_b (1-h) + G_{b0} G'_{b0} \gamma_a h \right] \qquad (3.3.2)$$

In equation (3.3), j_a is the amplitude of ac current density applied to section a, $s=j\omega$, and P_0, is the cw photon density. $\gamma_{a,b}$, are the damping rates corresponding to each section and defined as:

$$\gamma_{a,b} = \frac{1}{\tau_{sp,a,b}} + G'_{a0,b0}P_0 \qquad (3.4)$$

$\tau_{a,b}$, are the spontaneous carrier lifetimes in their related sections. The total optical gain then can be expressed as:

$$G_0 = G_{a0}(1-h) + G_{b0}h \equiv \frac{1}{\Gamma \tau_p} \qquad (3.5)$$

which is modified for the two-section gain-lever configuration. According to equation (3.3) the resultant response function has a cubic frequency dependence compared to that of the single-contact laser, which has a quadratic form.

The resonance frequency can be derived from equation (3.3) for modulation frequencies well above the damping rate in each section as [7]:

$$f_r^{\,2} = \frac{\Gamma P_0}{4\pi^2}[G_{a0}G'_{a0}(1-h) + G_{b0}G'_{b0}h] \qquad (3.6)$$

The applied current arrangement to each section defines the corresponding gain ratio for uniform pumping and gain-lever pumping cases. When the device is pumped uniformly the ratio of gain in each section to the total gain is equal to 1, or $\frac{G_{a0}}{G_0} = \frac{G_{b0}}{G_0} = 1$.

In this case the modulation response of the two-section has the same frequency dependence as the single section device. Based on this formulation, an increase in

modulation efficiency enhancement with constant resonance frequency was observed when the ratio of the gain in the modulation section to the total gain is less than 1 [7]. Also according to equation (3.6), the resonance frequency was found to be constant due to the parabolic-like shape of the gain characteristics in QW structures where, for moderate values of G_{a0}, G_{b0}, the products of gain and differential gain in the two-section are about identical, $G_{a0}G'_{a0} \cong G_{b0}G'_{b0}$. The resonance frequency was found to be the same as the uniformly-pumped condition for cases when the gain section occupies a large fraction of the cavity. Figure (3.2) shows the response curves for different values of normalized gain in the modulation section, or G_{a0}/G_0. As seen in this figure, the resonance frequency is fairly unchanged for different bias levels on the modulation section, but the modulation efficiency enhancement is larger for smaller values of this ratio [7].

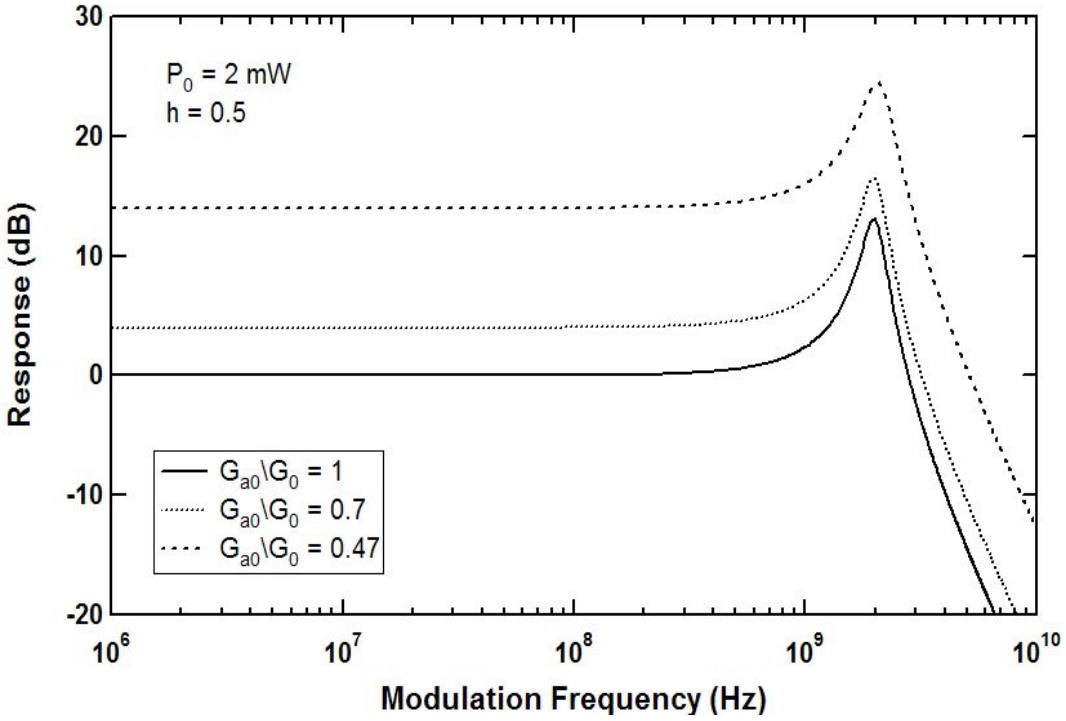

Figure (3.2) *Modulation responses for different pumping levels applied to the modulation section, N. Moore and K. Y. Lau, App. Phys. Lett., 55, 936 (1989)*

The modulation efficiency enhancement then was found from the relative modulation response which is the ratio of the modulation response, equation (3.3), to its corresponding value for the uniformly pumped case where $h=0$ and $f \rightarrow 0$ [7].

$$\eta = \frac{\frac{p}{i_a}(h)}{\frac{p}{i_a}(0)} = \frac{\gamma_b}{(1-h)\gamma_b \frac{G_{a0}}{G_0} + (h\gamma_a \frac{G'_{b0}}{G'_{a0}}) \frac{G_{b0}}{G_0}} \qquad (3.7)$$

when the gain section occupies most of the cavity length ($h \approx 1$), equation (3.7) reduces to:

$$\eta = \frac{\gamma_b}{\gamma_a} \frac{G'_{a0}}{G'_{b0}} \qquad (3.8)$$

In this expression, the ratio of the damping rate in each section can be approximated at low photon density to the inverse of the spontaneous carrier lifetime so that the modulation efficiency enhancement is described as:

$$\eta = \frac{\tau_a}{\tau_b} \frac{G'_{a0}}{G'_{b0}} \qquad (3.9)$$

At high photon density however, $\eta \rightarrow 1$, since $\frac{\gamma_b}{\gamma_a} \rightarrow \frac{G'_{b0}}{G'_{a0}}$.

According to equation (3.9) the modulation efficiency will be enhanced for the cases where the gain-lever effect produces a larger differential gain in the modulation section than the gain section ($G'_{a0} > G'_{b0}$).

Using the gain-lever effect, a modulation efficiency enhancement of 23 dB at a resonance frequency of f_r=3 GHz was demonstrated for a 220 μm long GaAlAs/GaAs single QW

laser at the expense of lower bandwidth and output power to a few GHz and few mW respectively [7].

In the QW gain-lever devices, the modulation bandwidth is found to be limited by the damping rates γ_a, γ_b, similar to the conventional single section lasers [10].

The Gain-lever effect has been also studied for frequency modulation of single QW lasers. It was shown that the frequency modulation is possible in the gain-levered laser structure due to the asymmetry in the gain and the linewidth enhancement factors in each section [9]. In related studies, an FM modulation efficiency enhancement of 22 GHz/mA was demonstrated without a corresponding increase in the FM noise [9]. The gain-lever frequency modulation technique requires extra consideration and different formulations which is outside the scope of this thesis.

In following chapter, the impact of the gain-lever effect on the QD laser diode which is demonstrated for the first time in this work, will be introduced. A novel formulation will be provided for the modulation response function which perfectly fits to the experimental data and can be used to determine the actual gain-lever value. Finally limiting factors and possible solutions will be discussed.

3.4 Chapter 3 References

[1] H. Olesen, et al., "Proposal of Novel Gain-Levered MQW DFB Lasers with High and Red-Shifted FM Response," *IEEE Photon. Technol. Lett.,* 5, 599 (1993)

[2] K. Y. Lau*,* "Gain-levered semiconductor laser-direct modulation with enhanced frequency modulation and suppressed intensity modulation," *IEEE Photon. Technol. Lett.,* **3**, 703-705, (1990)

[3] K. J. Vahala, M. A. Newkirik, and T. R. Chen, "The optical gain-lever: a novel gain mechanism in the direct modulation of QW semiconductor lasers," *Appl. Phys. Lett.,* 54, 2506, (1989)

[4] M. A. Newkirik, K. J. Vahala, "Parasitic-Free Measurement of the Fundamental Frequency Response of a Semiconductor Laser by Active-Laser Photomixing," *Appl. Phys. Lett.,* 52, 770 (1988)

[5] K. J. Vahala, M. A. Newkirk, *Proceeding of IEEE/LEOS,* (1988)

[6] M. A. Newkirk, K. J. Vahala, "Equivalent Circuit Model for Active-Layer Photo-mixing: Parasitic-Free Modulation of Semiconductor Lasers," *Appl. Phys. Lett.,* 53, 1141 (1988)

[7] N. Moore and K. Y. Lau, "Ultrahigh efficiency microwave signal transmission using tandem-contact single QW GaAlAs lasers," *Appl. Phys. Lett*., 55, 936 (1989)

[8] D. Gajic and K. Y. Lau, "Intensity noise in the ultrahigh efficiency tandem-contact QW lasers," *Appl. Phys. Lett*., 57, 1837 (1990)

[9] K. Y. Lau, "Frequency modulation and linewidth of gain-levered two-section single

QW laser," *Appl. Phys. Lett*., 57, 2068 (1990)

[10] M. Kuznetsov, A. E. Willner and I. P. Kaminow, "Frequency modulation response of tunable two-segment distributed feedback lasers," *Appl. Phys. Lett.,* 55, 1826-1828, (1989)

Chapter 4

QUANTUM DOT GAIN-LEVER LASER DIODE

4.1 Motivation for the QD Gain-Lever Laser

Analog direct modulation of semiconductor lasers is used in low-cost optical communication networks, which are typically connected through optical fiber links. It is usually desired to improve the performance and capacity of these optical networks by enhancing the modulation efficiency, providing high modulation bandwidth, low signal distortion, low relative intensity noise and reduced radio frequency link loss. The modulation bandwidth is often limited by the relaxation oscillation frequency of the laser. Unwanted signal distortions, such as inter-modulation distortions are usually caused due to the nonlinear coupling between electrons and photons and intrinsic frequency chirp in the semiconductor laser which results in output signal distortions. On the other hand, most of the limitations mentioned above are induced by some intrinsic parasitic effects such as non-linear gain suppression, carrier density dependent lifetimes of electrons and photons, carrier transport delay and frequency effects on the current injection efficiency (of which some of them are briefly reviewed in chapter 2). Although most of these limitations can be removed to some extent by using better materials and optimizing the device structure, the maximum improvement can be achieved by developing the

modulation techniques.

As described in previous chapters, semiconductor lasers have been substantially studied for high-speed modulation applications and their performance improved significantly by applying some novel modulation techniques such as using the gain-lever effect [1, 2, 3, 7, 8]. Previously, two-section QW lasers have been investigated theoretically and experimentally to explore the gain-lever phenomena [7, 8]. In these studies, an intensity modulation efficiency enhancement of 15 dB for a 400 μm QW laser and a 22 GHz/mA FM modulation efficiency enhancement were reported with no improvement in 3-dB bandwidth [7, 8].

In this work, it is suggested that the gain-lever QD laser diodes are extremely promising for high-speed optical communication systems due to their potential for strong gain saturation with carrier density, high differential gain and direct modulation with small chirp. As also discussed in chapter 3, the gain-lever effect can be realized better from the gain saturation standpoint since this effect directly benefits from the gain clamping and sub-linear relationship between the gain and the carrier density in different semiconductor materials. Gain saturation in QW materials was presented in a previous chapter. Here it is also necessary to look at the gain saturation in QD materials and compare it to that of the QWs, which leads us to realize the impact of gain-lever effect in QD lasers.

4.1.1 Gain Saturation in Quantum Dots

From chapter 3, we can recall that the optical gain increases by injecting excess carriers, and it is directly related to the density of states function of the semiconductor material which can be bulk, QW, or QD. As a result the available optical gain and its rate of change with carrier density is not the same for different structures. The density of states function in bulk materials is continuous and directly proportional to the square root of energy. In QWs, the density of states increases as a step-function compared to the bulk material, but the density of states in QDs is a δ-function in energy. Therefore, as is illustrated in figure (4.1), the optical gain vs. carrier density in QDs, first increases rapidly and then saturates faster than even in QWs and also the differential gain in QDs changes more with gain compared to QWs. Consequently, due to the strong gain saturation with carrier density and high differential gain in QD materials, devices fabricated from these novel materials are interesting for high speed applications.

In this thesis, an accurate gain model for QDs is presented, that can precisely predict the gain saturation in these materials. Also, the modulation efficiency enhancement in a p-doped QD gain-lever laser diode is studied for the first time. The 3-dB modulation bandwidth of the gain-lever QD laser is also examined and the relation between the normalized 3-dB bandwidth and the modulation section gain for different power levels is discussed. Using the rate equation analysis and small signal approximation, new theoretical equations describing the device's modulation response function are derived that matches better with the experimental data.

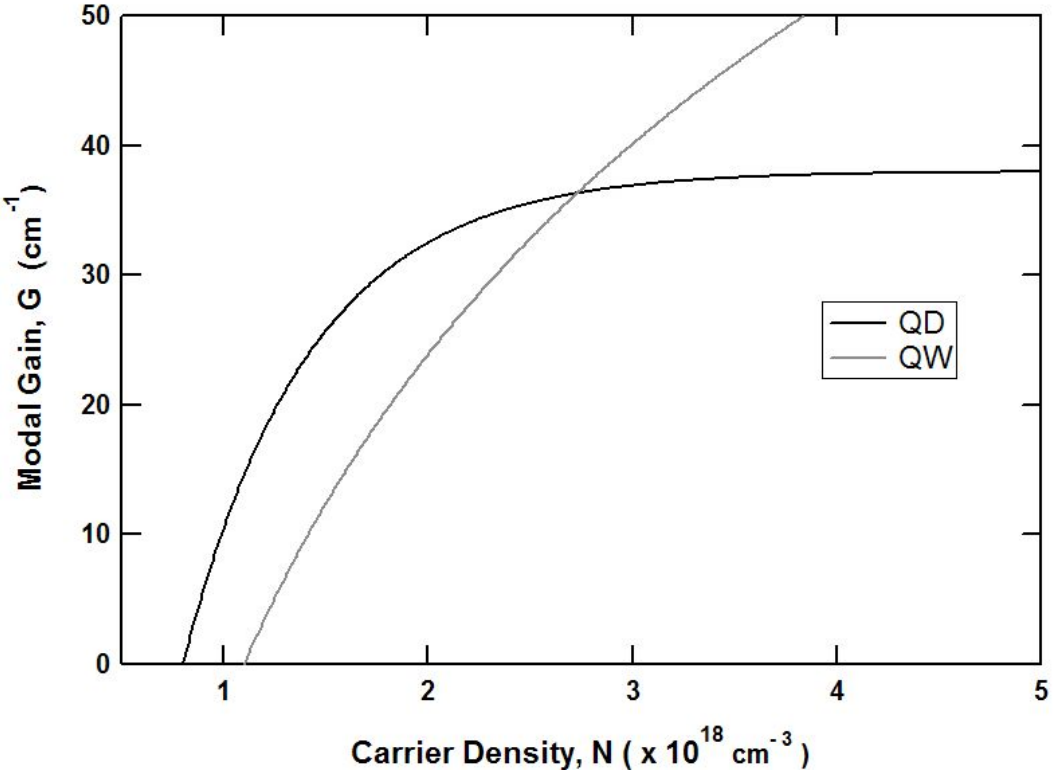

Figure (4.1) *A comparison of the variation of the material gains in Quantum Dot and Quantum Well as a function of carrier density*

4.2 Experimental Results

In this section the device structure, an accurate gain model for QD material, the experimental setup and finally the experimental results for the modulation efficiency enhancement of the gain-lever QD laser diode studied at CHTM, are presented.

4.2.1 Device Structure

The device under investigation was grown by the Molecular Beam Epitaxy (MBE) growth technique on an $\mathbf{n}^+$ (001) GaAs substrate. The active region consisted of 10 layers of InAs QDs covered 5 nm $In_{0.15}Ga_{0.75}As$ QWs in a DWELL structure. The QW layers are separated by 33 nm GaAs spacers of which 10 nm is carbon p-type doped. The device's cladding layers are step-doped 1.5 μm thick $Al_{0.35}Ga_{0.65}As$. The entire laser structure is then capped with a 400 nm thick C-doped GaAs [10]. Our QD laser chip is a multi-section laser that consists of three electronically isolated sections with a geometry of a 1.5 mm cleaved cavity length (the length of each isolated section is 0.5 mm), and a 3 μm wide ridge waveguide fabricated by standard processing techniques. Two of the three sections are wire-bonded together through a separate metal contact pad in order to use the device in a two-section (gain-lever) configuration.

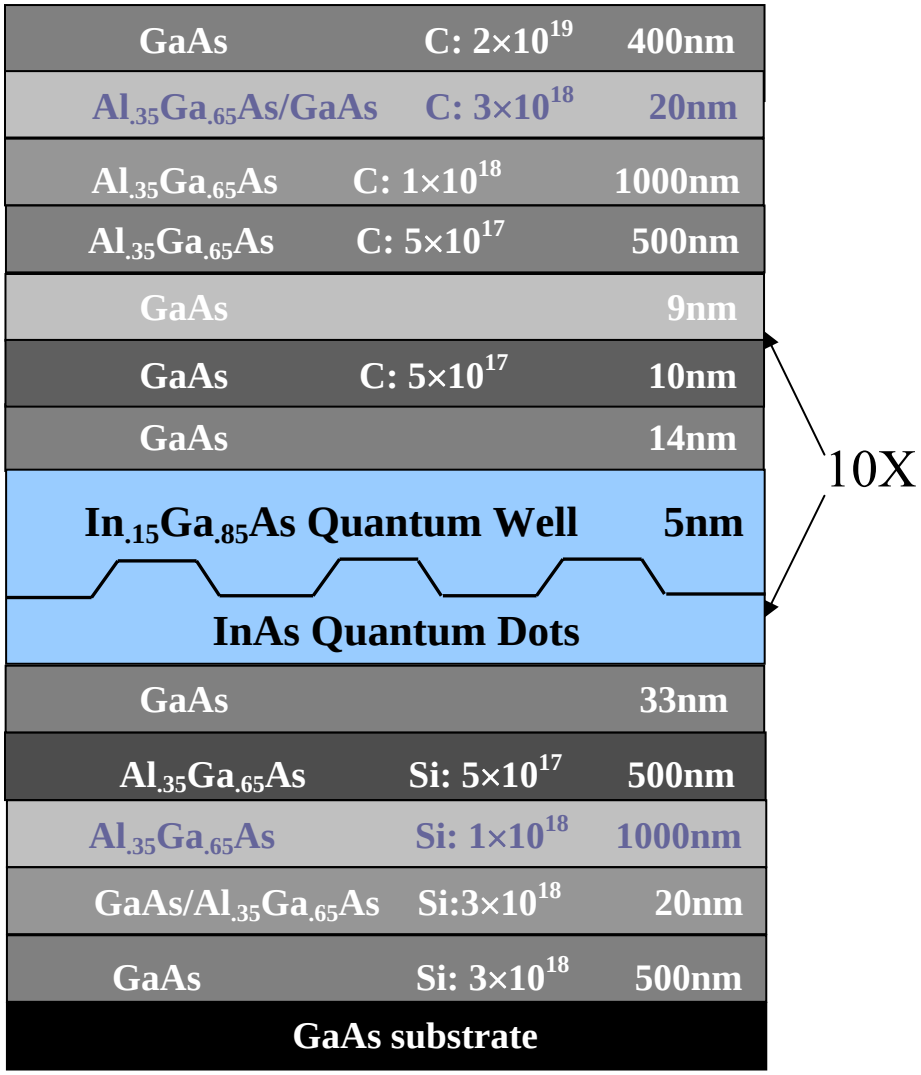

Figure (4.2) *Schematic layer diagram of the 10-stack InAs/InGaAs DWELL laser structure under the investigation*

4.2.2 Device Characteristics and QD Gain Model

The modulation experiment was done on a 1.5-mm long device having a threshold current of 35.5 mA and a peak wavelength of 1290 nm under uniform pumping conditions. Figure (4.3.a) shows the *P-I* characteristics of the device.

In order to characterize the gain-lever effect in this device, gain values in each section as a function of the bias currents are desired, and, therefore, an accurate QD gain model is needed. We chose to derive the relation between current density and gain from the measured threshold current densities and efficiencies of broad area lasers with different cavity lengths. For this purpose, first the differential quantum efficiency, η_d, is calculated from the slope efficiency expression which is defined as:

$$\eta_d = (\frac{q}{h\upsilon})\frac{dP}{dI} \qquad (4.1)$$

where *dP/dI* is the slope efficiency and can be obtained from the *P-I* curve for currents above the threshold, $I>I_{th}$. The differential quantum efficiency is the measure of the efficiency with which light output increases with an increase in the injection current and is also related to the cavity length through the injection efficiency, η_{inj}, internal loss, α_i, and mirror reflectivity, *R*, as the following expression:

$$\frac{1}{\eta_d} = \frac{1}{\eta_{inj}}\left(1 - \frac{\alpha_i L}{\ln(R)}\right) \qquad (4.2)$$

Based on equation (4.1), the differential quantum efficiencies of some broad area lasers (cleaved from the same wafer) with different cavity lengths of 0.75, 1, 1.5, 2, 2.5, 3 mm,

a)

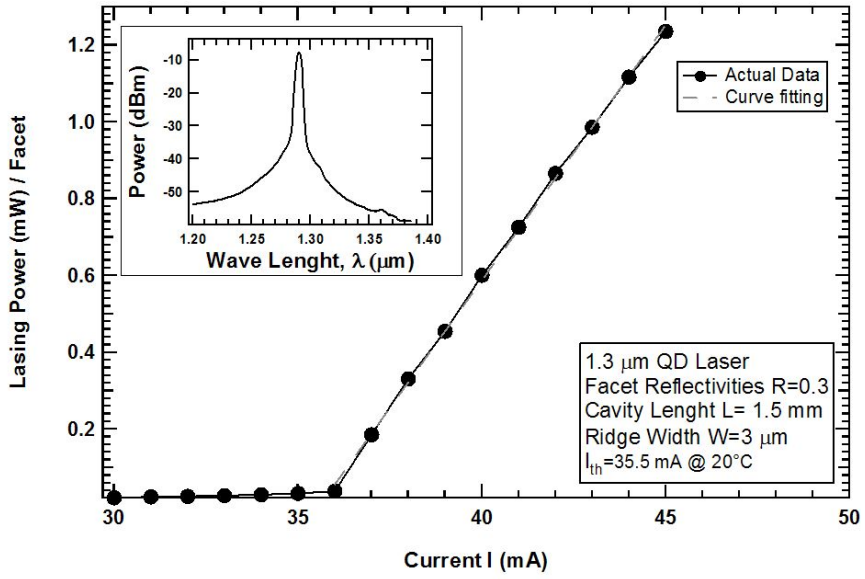

b)

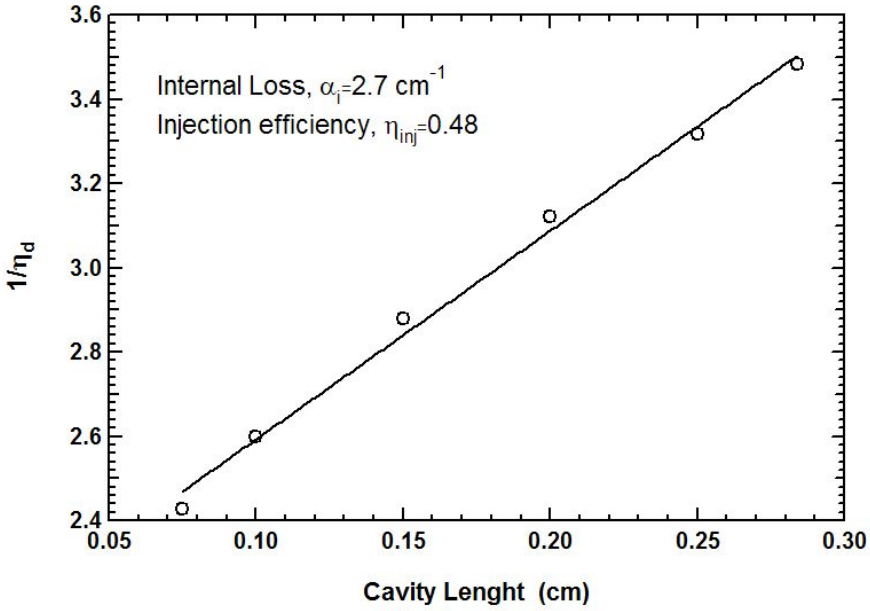

Figure (4.3) *a) P-I curve and lasing spectrum of the two-section QD device under investigation and b) the differential quantum efficiency inverse as a function of cavity length, curve-fitted with equation (4.2)*

were measured and then $1/\eta_d$ was plotted versus cavity length and curve-fitted with equation (4.2) as shown in figure (4.3.b). As illustrated in this figure, the resultant fitting parameters give the values for internal loss of, α_i=2.7 cm^{-1} and internal efficiency of, η_i=0.48. Finally, the threshold gains, G_{th}*'s*, are calculated from $G_{th} = \alpha_i + \alpha_m$, by finding the corresponding mirror loss for different cavity lengths from $\alpha_m = \frac{1}{L}\ln\left(\frac{1}{R}\right)$. In figure (4.4), calculated threshold gains are plotted versus threshold current densities. To obtain the maximum gain value possible as a function of the pump current it is necessary to curve-fit this data with an accurate gain model.

Equation (4.5) is a simple empirical gain model with exponential threshold current density dependence which was used to describe the gain saturation in QD materials [9]:

$$G = G_{\max}\left(1 - \exp(-\ln 2(\frac{J}{J_{tr}} - 1))\right) \qquad (4.5)$$

where G_{max} is the maximum gain for ground state lasing in the quantum dot media, and *J,* J_{tr} are the threshold and transparency current densities, respectively. However the strong gain saturation with current density behavior in dots can be more accurately modeled by a square-root current density dependence as was first described by our research group [6], which is to say:

$$G(J) = G_{\max}\left[\frac{2\sqrt{J}}{\sqrt{J} + \sqrt{J_{tr}}} - 1\right] \qquad (4.6)$$

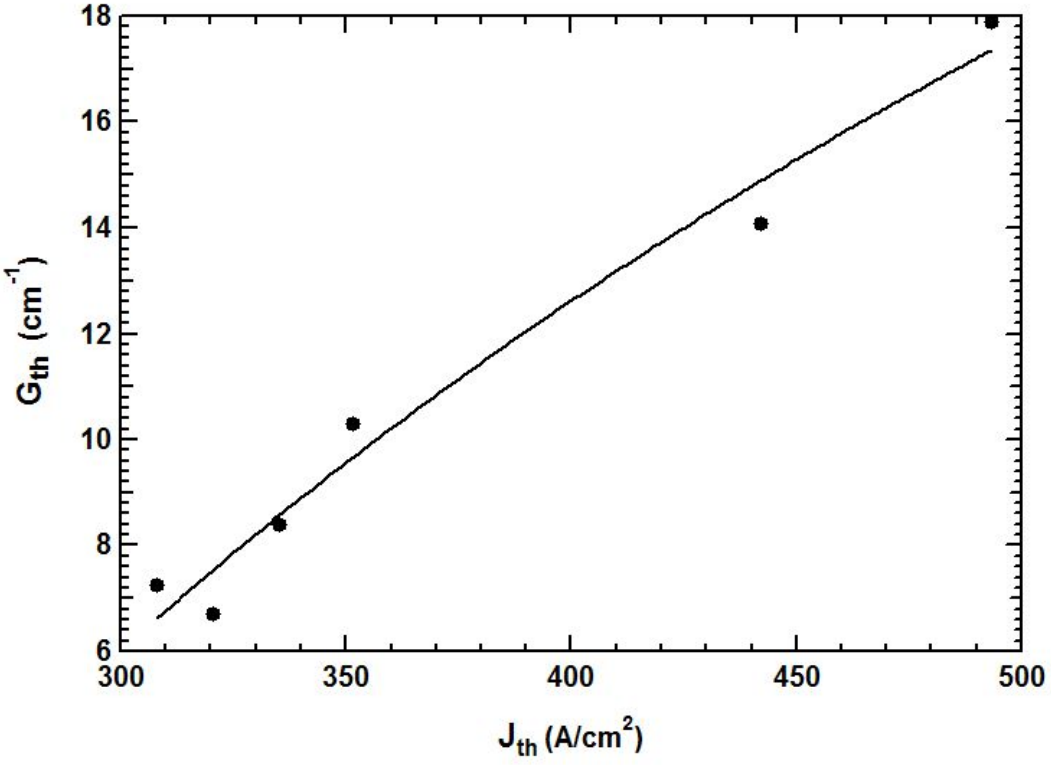

Figure (4.4) *Threshold gain as a function of threshold current density at room temperature*

Calculated data shown in Figure (4.4) were then curve-fitted with the square root gain model given in equation (4.6). Surprisingly as illustrated in the figure, the gain does not saturate as strongly as expected. Part of the reason is that we are examining gain values that are well below the maximum gain. From the curve fitting results a maximum gain of G_{max}=92.8 cm^{-1} was calculated for the p-doped QD material under the investigation.

4.2.3 Modulation Characteristics

Recall from chapter 3 that the gain-lever effect is based on the sub-linear relationship between the optical gain and carrier density (which can be also approximated by gain vs. injected current density). Figure (4.5.a) shows the schematic view of a typical gain versus carrier density characteristic of a two-section QD laser [7].

Under forward bias and non-uniform pumping, the device exhibits the gain-lever effect. In this case, the longer section (the "gain section") is biased at a high gain level, G_{b0}, and the shorter section (the "modulation section") is biased at low gain G_{a0}, where h is the fractional length of the gain section. As seen in Figure (4.5.a) the modulation section provides high differential gain, G'_a, under small signal RF modulation and the gain section which occupies a large fraction of the cavity supplies most of the gain at a relatively smaller differential gain, G'_b. Since the total modal gain is clamped at threshold, (neglecting the power coupled into the lasing mode due to spontaneous

a)

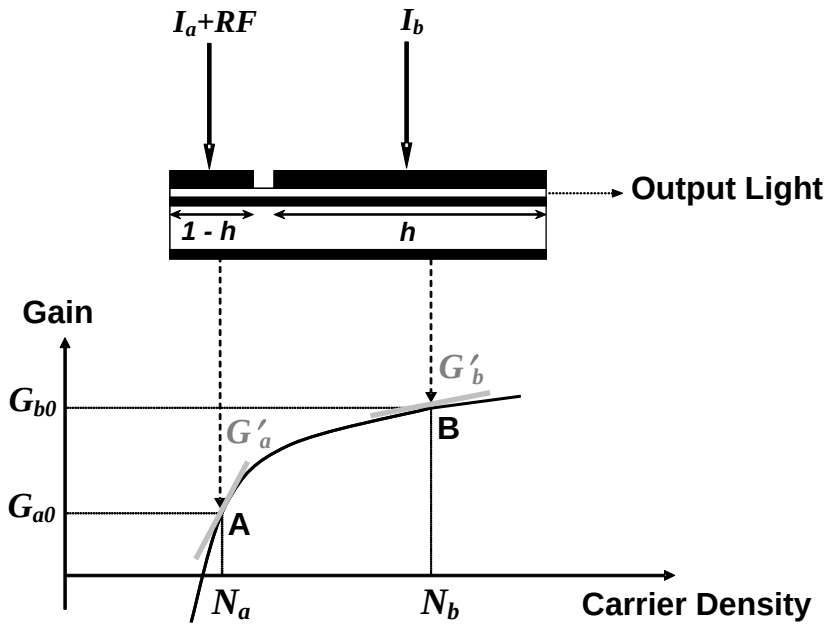

b)

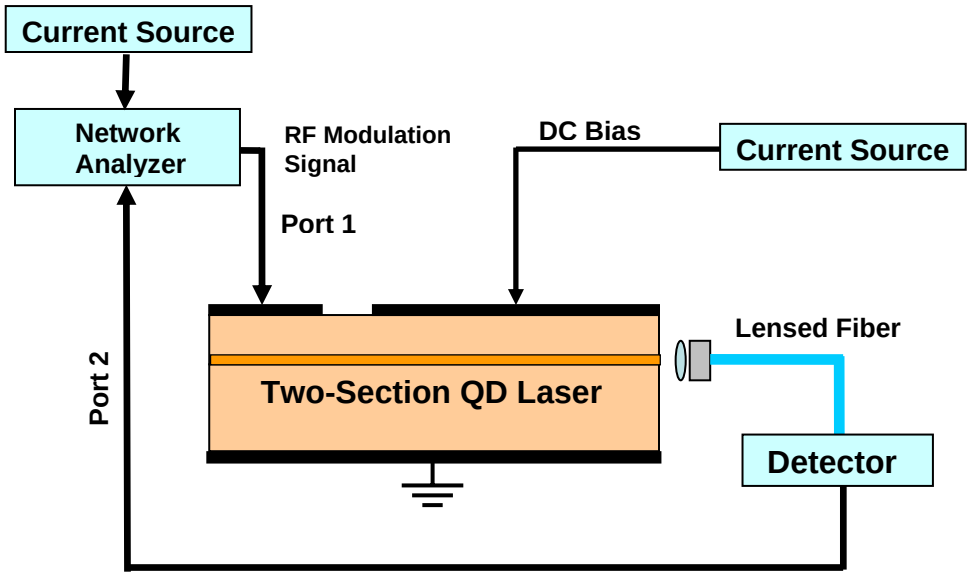

Figure (4.5) *a) Schematic diagram of a two-section quantum dot laser with gain versus carrier density curve showing bias points for both sections and b) the schematic view of the experimental setup*

emission) and according to the non-linear dependence of gain with carrier density, a small change in carrier density in the modulation section produces a much larger variation in carrier density in the gain section [7]. In another words, one can obtain a large change in the carrier density in the gain section by applying a small change in injection current in the modulation section. In such a case, the RF optical gain will increase due to the gain-lever when the differential gain in the modulation section, G'_a, is greater than the differential gain in the gain section, G'_b. In order to obtain a stronger gain-lever effect, the device operation point is chosen such that the resultant differential gain ratio G'_a / G'_b is as high as possible.

4.2.4 Experimental Setup

The high-speed experimental setup used in this research is shown in figure (4.5.b). The laser chip is attached using indium to a separate "C-mount", which is bonded to a copper sub-mount located on a TE-cooler that stabilizes the desired operation temperature. Two accurate (low noise) current sources are used to provide the current flow into each section. The gain section is directly biased using a typical probe station. The RF modulation signal is provided by a HP8722 network analyzer through port 1. Before performing each measurement the network analyzer is calibrated to subtract the noise induced through the input and output ports. The output light is then collected by a single mode lensed fiber with 10% coupling efficiency and transferred to a 40 GHz, high-

speed New Focus photodetector that is connected to the network analyzer through port 2. Finally the modulation response produced at the network analyzer is taken from the corresponding transmission coefficient S_{21}.

4.2.5 Modulation Efficiency Enhancement

The modulation efficiency enhancement was measured by comparing the modulation responses for uniform and asymmetric pumping cases. For uniform pumping the two sections are biased such that they have equal current density. The asymmetric pumping situation corresponds to the case where the two sections have different current densities. Specifically, the current injection into the modulation section is decreased, while the current into the gain section is increased to maintain an output optical power equal to the uniformly pumped condition. Equal output power or equivalently photon density is considered to be the valid experimental condition for comparisons of different pumping scenarios.

The enhancement in the AM response for the modulation applied to the short section is proportional to the ratio of the differential gain in each section. Consequently, the device operating point, which is influenced by the length of each section, is chosen to give a differential gain ratio as high as possible to increase the modulation efficiency. Another way to look at this strategy is that we want the pump asymmetry to be as large as possible. Intuitively, this situation arises when $G_{a0} = 0$. To know the differential gain

ratio, then it is clear from figure (4.5.a) that we also have to know G_{a0} and G_{b0}.

In fact these two parameters are fundamental to the laser action so that the asymmetrical pumping is usually characterized in terms of one or the other. For this work, we choose Moore and Lau's convention, which is to specify G_{a0}, the threshold gain in the modulation section.

For the gain-lever condition, assuming a constant photon density in the cavity, the gain in each section is found from the ratio of the stimulated emission rates and the gain model according to Equation (4.6) as:

$$G_{a0} = \frac{G_a(J_a)G_{th}}{hG_b(J_b) + (1-h)G_a(J_a)} \qquad (4.7.1)$$

$$G_{b0} = \frac{G_b(J_b)G_{th}}{hG_b(J_b) + (1-h)G_a(J_a)} \qquad (4.7.2)$$

where, G_{a0}, G_{b0} are the threshold gains in the shorter (a) and longer sections (b) respectively, G_a ,G_b are the unclamped gains in the respective sections, G_{th} is the total threshold modal gain of the device and h is the fractional length of the gain section and is equal to 2/3 or 0.67 for this experiment. The relation between the threshold gains in each of the two sections is also related to the total threshold modal gain as [7]:

$$\Gamma\left[hG_{b0} + (1-h)G_{a0}\right] = G_{th} \equiv \alpha_i + \alpha_m \qquad (4.7.3)$$

where the threshold gains in each section are individually a function of current density in the related sections, $G_{a0}(J_a)$, $G_{b0}(J_b)$.

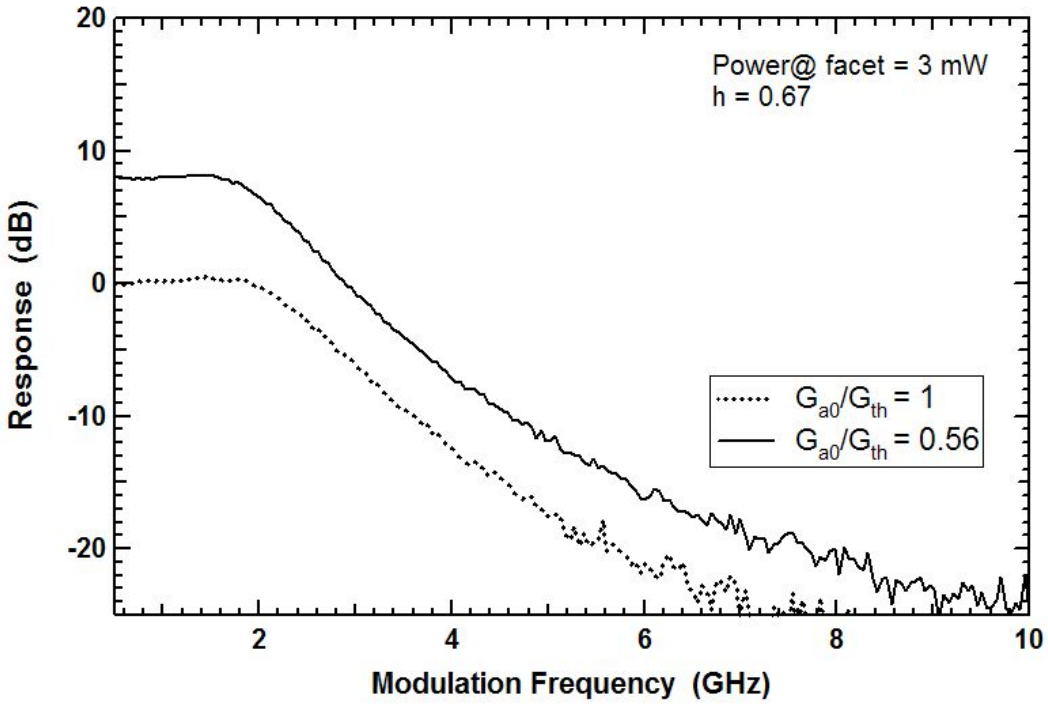

Figure (4.6) *Modulation responses for uniform and asymmetric pumping cases in the two-section QD laser*

In figure (4.6), modulation responses for the uniform and asymmetric pumping cases at a constant power level of 3 mW/facet are plotted. A modulation efficiency enhancement as high as 8-dB was observed for our two-section QD device when the shorter section was biased such that G_{a0}/G_{th}=0.56 (note: G_{a0}/G_{th}=1 corresponds to the uniform pumping case). According to previous research on the modulation efficiency enhancement [7]:

$$\eta = \frac{\eta_{gainlever}}{\eta_{uniform}} = \frac{\tau_a}{\tau_b}\frac{G'_{a0}}{G'_{b0}} \qquad (4.8)$$

Making the reasonable assumption that the carrier lifetimes τ_a and τ_b are the same due to the p-doping of the QDs, the 8-dB improvement in η corresponds to a differential gain ratio of 2.5. At this point it is noted that equation (4.8) assumes low photon density, where the damping rates are dominated by the carrier lifetime terms and that the fractional gain section length h approaches 1, which is not the case for our QD gain-lever device. A new and improved method for extracting the gain-lever value from RF modulation experiments will be explored in section 4.3.

4.2.6 3-dB Modulation Bandwidth

In our experiment the 3-dB modulation bandwidth varies between 2-5 GHz for an output power range of 3-14 mW at the facet under uniform bias. Generally, as output power increases the absolute bandwidth will increase in the two-section laser just as in the single-section laser diode. For the two-section laser, however, it is more instructive to

analyze the normalized bandwidth. In Figure (4.7), the normalized 3-dB bandwidth is plotted as a function of gain in the modulation section, G_{a0}, for three different power levels. Each set of f_{3dB} data were measured under gain-lever conditions that have a constant output power with f_{3dB0} corresponding to the bandwidth for the uniform pumping case. Equations (4.6), (4.7.1) and (4.7.2) are then used to calculate the threshold gains G_{a0} and G_{b0}. The results show that the modulation bandwidth decreases with more asymmetric pumping for this particular p-doped two-section QD laser. Also the bandwidth becomes more power dependent with increasing pump asymmetry or, alternatively, lower threshold gain, G_{a0}, which is probably evidence of non-linear gain suppression. Overall, these trends are not desirable results, so we would like to understand the modulation response of a two-section laser in greater depth. This is the primary goal of the remaining sections of this thesis.

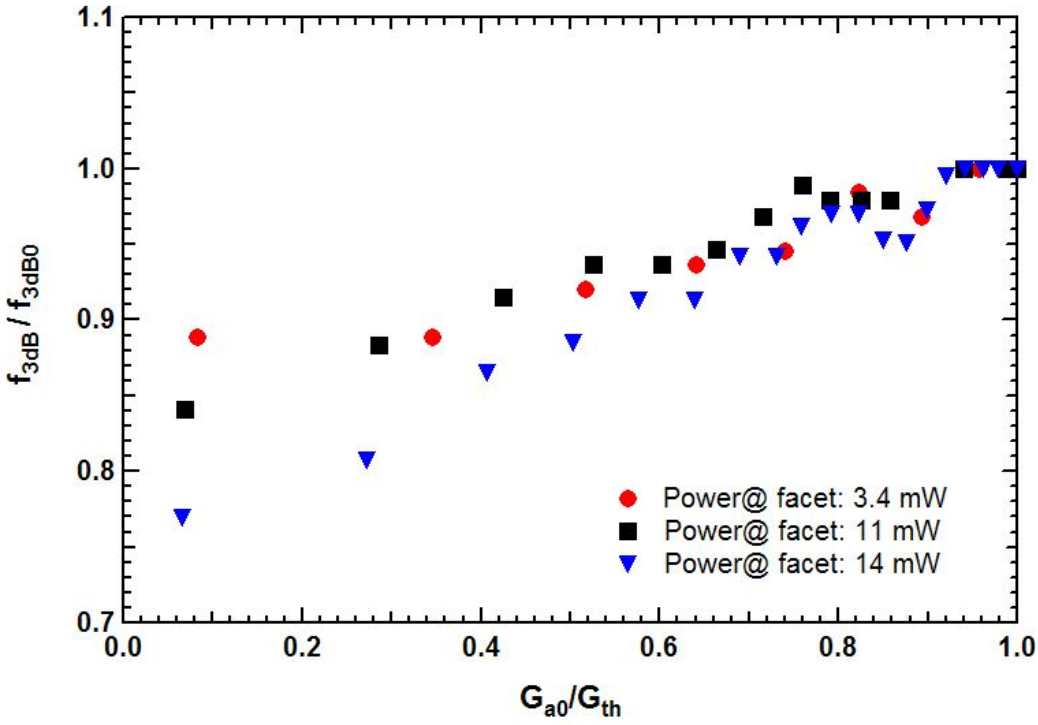

Figure (4.7) *Normalized 3-dB bandwidth as a function of gain in the modulation section*

4.2.7 Modulation Response Function for Single-Section Lasers

The modulation responses from the gain-lever experiment were also curve-fitted with the single-section modulation response equation expressed below to extract the resonance frequencies related to each response [8]:

$$|M(f)|^2 \propto \frac{1}{1+(2\pi f\tau_c)^2}\frac{f_r^{\,4}}{\left[(f_r^{\,2}-f^2)^2+(\frac{\gamma_{uni}}{2\pi})^2 f^2\right]} \qquad (4.9)$$

In equation (4.9), f_r, is the resonance frequency, γ_{uni}, is the damping factor of the uniformly pumped laser and τ_c is the carrier transport time. The uniform damping rate, γ_{uni}, can be defined as:

$$\gamma_{uni} = \frac{1}{\tau_{sp}} + 4\pi f_r^{\,2}\tau_p = \frac{1}{\tau_{sp}} + G'P_0 \qquad (4.10)$$

where τ_{sp} is spontaneous carrier lifetime, G' is differential gain, τ_p, corresponds to photon lifetime and P_0 is the photon density. Figure (4.8) shows the normalized resonance frequency (extracted from curve fitting) as a function of normalized gain in the modulation section. The resonance frequency increases at higher powers (higher photon densities), since it is directly proportional to the photon density. In figure (4.8) the sudden increase in the resonance frequency for values below $G_{a0}/G_{th} = 0.4$, seems to be totally unphysical. Therefore, according to the results, it is concluded that for values below $G_{a0}/G_{th} = 0.4$, the conventional single-section model is no longer valid for the two-section configuration.

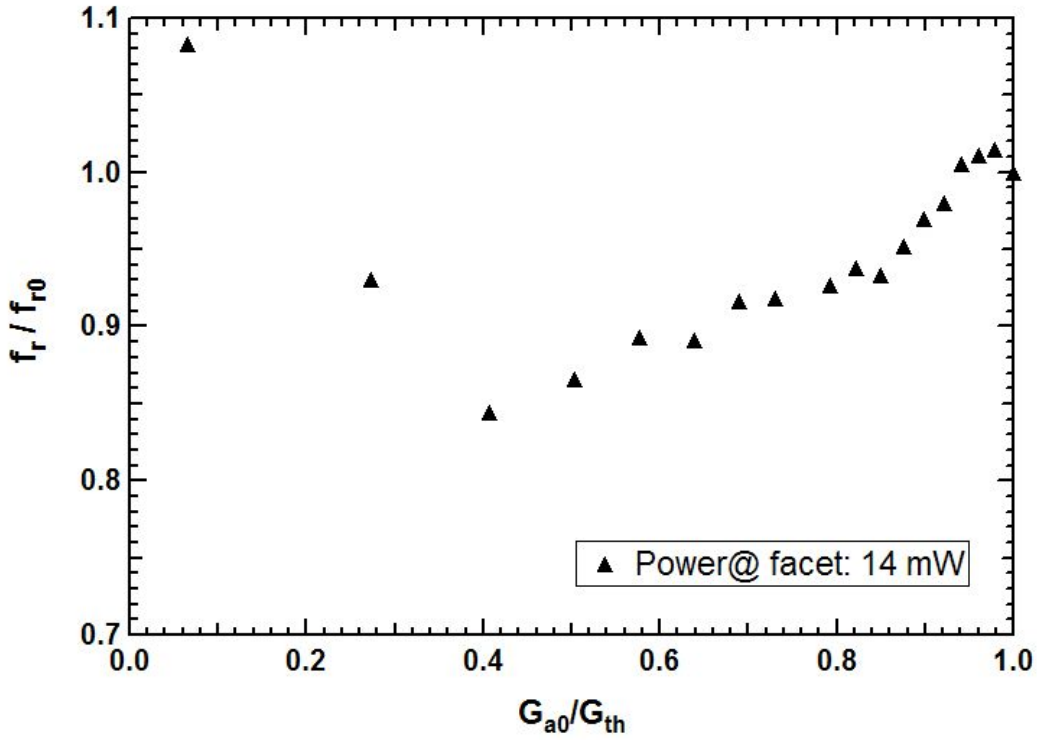

Figure (4.8) *Normalized resonance frequency as a function of gain in the modulation section plotted based on the single-section model*

As seen in the conventional single section response function, equation (4.9), only one term is included to describe the damping rate, which is defined as equation (4.10). The main problem arises from the fact that the damping rates in the two-sections are not equal due to the different current densities applied to each section.

As was explained before, in the gain-lever bias configuration, the modulation section is biased at a low gain level (which corresponds to high differential gain value) and the longer section is biased at higher gain that corresponds to low differential gain. In this case, however, the damping rates have different values in each section due to different differential gains due to the asymmetry. In another words, as the normalized modulation section gain, G_{a0}/G_{th}, decreases, the modulation section's damping rate, γ_a, increases while the damping rate in the gain section, γ_b, decreases. Therefore, a better model for the two-section device is desired that would account for different damping rates in each section.

4.3 Novel Two-Section Modulation Response Model

Using the relevant equations from chapter 3, the relative modulation response is found to be:

$$R(\omega) = \frac{\dfrac{p_m(\omega)}{j_a(\omega)}}{\dfrac{p_m(0)}{j_a(0)}} = \frac{A_2(i\omega + \gamma_b)}{-i\omega^3 - (\gamma_a + \gamma_b)\omega^2 + i\omega A_1 + A_2} \qquad (4.11)$$

As shown in equation (4.11) the modulation response function for a two-section laser has cubic frequency dependence unlike the single-section form which has quadratic frequency dependence. Also in this equation the two different damping rates are included to describe the damping effect on the resonance frequency and modulation response. The damping rates γ_a and γ_b can be related to the carrier lifetime, photon density and differential gain in the related section as:

$$\gamma_a = \frac{1}{\tau_a} + G'_{a0}P_0 \qquad (4.12.1),$$

$$\gamma_b = \frac{1}{\tau_b} + G'_{b0}P_0 \qquad (4.12.2)$$

In these expressions, the inverse carrier lifetimes correspond to the spontaneous damping term and the product of the photon density and differential gains represent the stimulated damping term. As mentioned before, at low photon density, the damping rates are dominated by carrier lifetimes. On the other hand, lower photon density (lower optical power) is not desired since the relaxation frequency and 3-dB bandwidth are small. The

interesting case is actually that of high photon density.

Under a high photon density condition the stimulated damping terms expressed in equations (4.12.1) and (4.12.2) are much larger than the spontaneous damping terms, and therefore, the first terms related to carrier lifetimes $\tau_{a,b}$, can be neglected in the damping rate expressions:

$$\gamma_a \approx G'_{a0} P_0 \qquad (4.13.1),$$

$$\gamma_b \approx G'_{b0} P_0 \qquad (4.13.2)$$

As was mentioned before, in order to obtain a stronger gain-lever effect, the device operation point is chosen such that the resultant differential gain ratio G'_{a0} / G'_{b0} is as high as possible. Furthermore, as indicated in equations (4.13.1), and (4.13.2), **under a high photon density condition, the damping rate ratio is the gain-lever**. Stated mathematically:

$$Gain\ Lever = \frac{\gamma_a}{\gamma_b} = \frac{G'_{a0}}{G'_{b0}} \qquad (4.14),$$

$$\eta = \frac{G'_a}{G'_b}\frac{\gamma_b}{\gamma_a}\frac{G_{th}}{G_{bo}} \approx \frac{G_{th}}{G_{bo}} \qquad (4.15)$$

where we have also included the new and more accurate expression for the modulation efficiency when the carrier lifetime terms are negligible in the damping rates [8]. Note that the modulation efficiency increase actually trends towards 1 under high photon density and large pumping asymmetry because G_{b0} is comparable to G_{th}. Thus the only true way to measure the gain-lever in this instance is by measuring the modulation

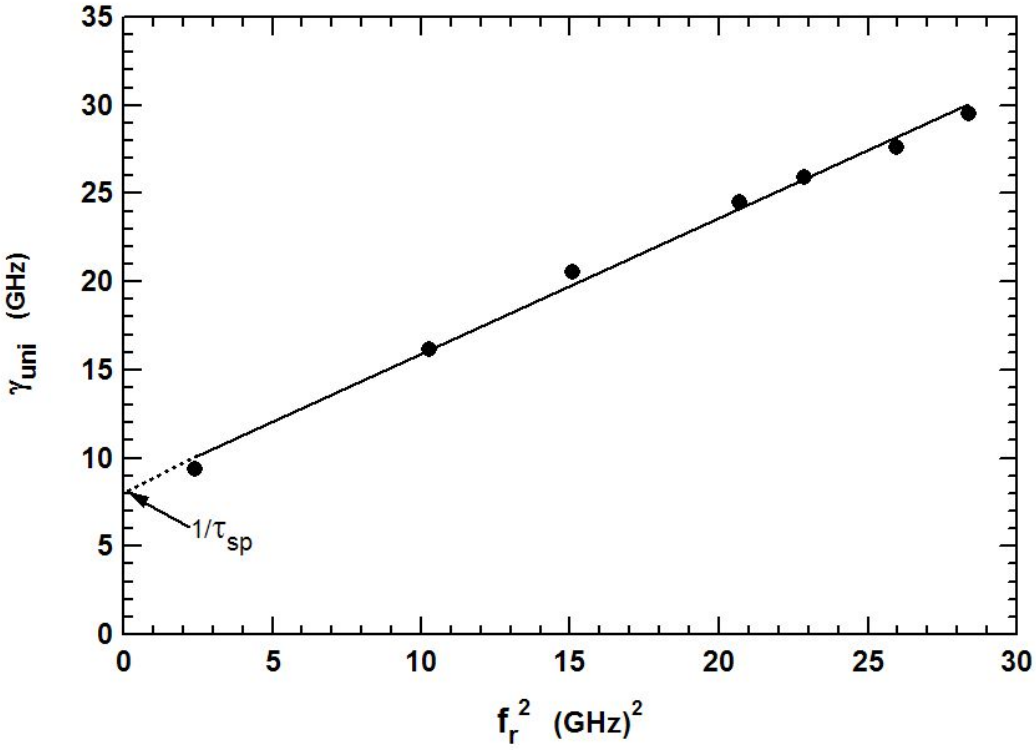

Figure (4.9) *Damping rate under uniform pumping case as a function of resonance frequency squared*

response and extracting the two damping rates.

To obtain a general idea of how good the approximation in (4.13.1) and (4.13.2) is in our p-doped QD lasers, we studied the change in the damping rate γ_{uni}, of the device under uniform pumping as a function of the relaxation frequency squared according to (4.10). The data is plotted in Figure (4.9). The inverse carrier lifetime, $1/\tau_{sp}$, can be extracted from this damping rate data at small relaxation oscillation frequencies. From the y-axis intercept of this graph, a value of 8 GHz for $1/\tau_{sp}$ corresponding to 0.12 ns for the spontaneous carrier lifetime is found. This value is relatively small compared to the typical carrier lifetime values (τ_{sp} is typically~1 *ns*). However, since the carrier lifetime decreases with doping level, this value is not too surprising in our p-doped QD device. In the ideal gain-lever case as we move toward more asymmetric pumping, the differential gain in the modulation section increases, and therefore γ_a, increases and γ_b, should decrease. In our p-doped device, the damping rate in the gain section, γ_b, does not decrease as much as desired under asymmetric pumping due to the small carrier lifetime. In other words, the damping rate in the gain section *b* hits a floor that inhibits the levering action.

Theoretically under the high photon density assumption, non-linear gain suppression can also impact the damping rate and hinder the gain-lever. From standard laser theory including non-linear gain, the damping rate expressions in equations (4.12.1) and (4.12.2) change to equation (4.16) and their ratio can be expressed as (4.17).

$$\gamma_{a,b} = \frac{1}{\tau_{a,b}} + \left(G'_{a0,b0} + \frac{\varepsilon}{\tau_p} \right) P_0 \qquad (4.16),$$

$$\frac{\gamma_a}{\gamma_b} = \frac{\left(G'_{a0} + \frac{\varepsilon}{\tau_p} \right)}{\left(G'_{b0} + \frac{\varepsilon}{\tau_p} \right)} \qquad (4.17)$$

where, ε, is the non-linear gain parameter. Thus, in the limit of a large non-linear gain effect or a small photon lifetime (a short cavity length), the gain-lever in (4.17) could entirely disappear, i.e. γ_a/γ_b approaches 1.

Despite these cautions on the possible limitations to the gain-lever effect, we know that the data in Figure (4.8) shows that the single-section modulation response equation fails for G_{a0}/G_{th} less than 0.4. Then it is justified to examine the modulation response function for a two-section device, equation (4.11), under the high photon density approximation. As discussed above, at high photon density, the carrier lifetimes in the two sections can be neglected and the damping rate equations reduce to (4.13.1) and (4.13.2). Now, by using the new expressions for damping rates, and neglecting the non-linear gain saturation effect for simplicity, the parameters A_1 and A_2 which were defined before in chapter 3 in equations (3.3.1) and (3.3.2), change to the following:

$$A_1 = \omega_r^{\,2} + \gamma_a \gamma_b \qquad (4.18.1),$$

$$A_2 = \frac{\gamma_b \gamma_a}{\tau_p} \qquad (4.18.2)$$

where, ω_r is the resonance frequency and is defined as [7]:

$$\omega_r = \sqrt{\Gamma P_0 \left[G_{a0} G'_{a0} (1-h) + G_{b0} G'_{b0} h \right]} \qquad (4.19)$$

And the photon lifetime, τ_p, which has already been defined is:

$$\frac{1}{\tau_p} = \Gamma \left[h G_{b0} + (1-h) G_{a0} \right] \qquad (4.20)$$

Substituting equations (4.18.1) and (4.18.2) into the relative modulation response, equation (4.11), and squaring its absolute value yields an expression for the relative modulation response as a function of angular frequency as follows:

$$\left| R(\omega) \right|^2 \propto \frac{\frac{\gamma_a^{\,2}}{\tau_p^{\,2}} (\gamma_b^{\,2} + \omega^2)}{\left[\frac{\gamma_a \gamma_b}{\tau_p} - (\gamma_a + \gamma_b) \omega^2 \right]^2 + \left[(\omega_r^{\,2} + \gamma_a \gamma_b) \omega - \omega^3 \right]^2} \qquad (4.21)$$

This is the most important result of this thesis. The modulation response function is usually expressed in terms of the frequency, f, and so using $\omega = 2\pi f$, equation (4.21) changes to:

$$\left| R(f) \right|^2 \propto \frac{\left(\frac{\gamma_a \gamma_b}{8\pi^3 \tau_p} \right)^2 \left(1 + \left(\frac{2\pi f}{\gamma_b} \right)^2 \right)}{\left[\frac{\gamma_a \gamma_b}{8\pi^3 \tau_p} - (\gamma_a + \gamma_b) \frac{f^2}{2\pi} \right]^2 + \left[\left[f_r^{\,2} + \frac{\gamma_a \gamma_b}{4\pi^2} \right] f - f^3 \right]^2} \qquad (4.22)$$

where, f_r, the resonance frequency can be defined as:

$$f_r = \frac{1}{2\pi} \sqrt{\Gamma P_0 [G_{a0} G'_{a0} (1-h) + G_{b0} G'_{b0} h]} \qquad (4.23)$$

Equation (4.22) is the relative modulation response function derived for a two-section laser diode. As indicated in this expression, the denominator is a cubic equation as opposed to that of the single-section device which has a quadratic dependence. Figure (4.10), presents the measured modulation response at an asymmetric pumping case ($G_{a0}/G_{th}=0.5$) which is curve-fitted with the one and two-section model, equations (4.9) and (4.22), respectively. The fitting parameters are the damping rates, γ_a, γ_b and the resonance frequency, f_r, while the constant photon lifetime, τ_p, is calculated from the device parameters. Recall that the photon lifetime is related to the total loss and threshold modal gain as:

$$\frac{1}{\tau_p} \equiv G_{th} = \left[\alpha_i + \frac{1}{L}\ln(\frac{1}{R})\right] v_g = \alpha_{tot} v_g \qquad (4.24)$$

The group velocity v_g is defined as, $v_g = \frac{c}{n}$ where c is the velocity of light in free space and n is the refractive index of the active region material (~*3.4* for GaAs). The internal loss of α_i=2.7 cm^{-1} and the mirror loss of α_m =7.2 $cm^{-1}$was found before for the 1.5-*mm* long QD device. Therefore by calculating the total loss as $\alpha_{tot} = \alpha_i + \alpha_m \approx 10$ cm^{-1}, and using equation (4.24), the corresponding photon lifetime can be found from the following expression:

$$\tau_p = \frac{n}{c\alpha_{tot}} \qquad (4.25)$$

Equation (4.25) yields a photon lifetime of $\tau_p \approx 10$ *ps* for the 1.5-*mm* QD device.

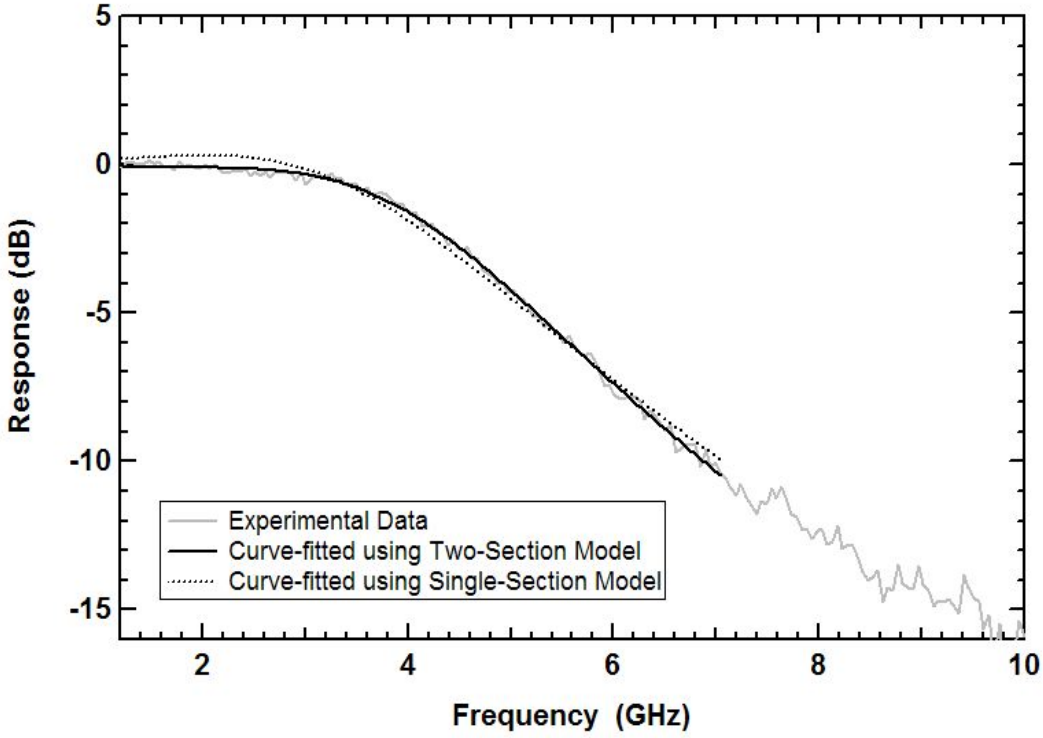

Figure (4.10) *Measured modulation response for the asymmetric pumping case* ($G_{a0} / G_{th} = 0.5$) *curve-fitted with one and two-section modulation response models*

The resultant curve fitting presented in figure (4.10), verifies that the new two-section response function fits better with the experimental data compared to that of the single-section response function.

According to the results illustrated in figure (4.8), we concluded that for values below $G_{a0}/G_{th} = 0.4$, the conventional single-section model is no longer valid for the two-section configuration. At this point, actual modulation responses curve fitted with the two-section model for different pump levels and the corresponding resonance frequencies were obtained from resultant fitting parameters. Figure (4.11.a), illustrates the variation of normalized resonance frequency f_r / f_{r0} as a function of normalized gain in the modulation section, G_{a0}/G_{th}, re-plotted this time by using the two-section response model. This figure verifies that the new response model does not fail for the different pumping asymmetries. Furthermore, according to equation (4.23), since the resonance frequency f_r, remains almost the same for different pumping values at the same output power, the gain-differential gain product in the two sections must be staying relatively constant, i.e., $G_{a0}G'_{a0} \cong G_{b0}G'_{b0}$. We believe that this result is due to the parabolic shape of the p-doped QD gain characteristics. Moore and Lau observed similar behavior in QW gain-lever laser diodes [7].

Figure (4.11.b) plots the damping rates in each section according to equation (4.22) and verifies that γ_a increases and γ_b decreases with increasing pump asymmetry (G_{a0}/G_{th} going from 1 towards 0) because G'_{a0} is increasing and G'_{b0} is decreasing as intended. The gain-lever varies between 1 and 2.3, which is generally consistent with the

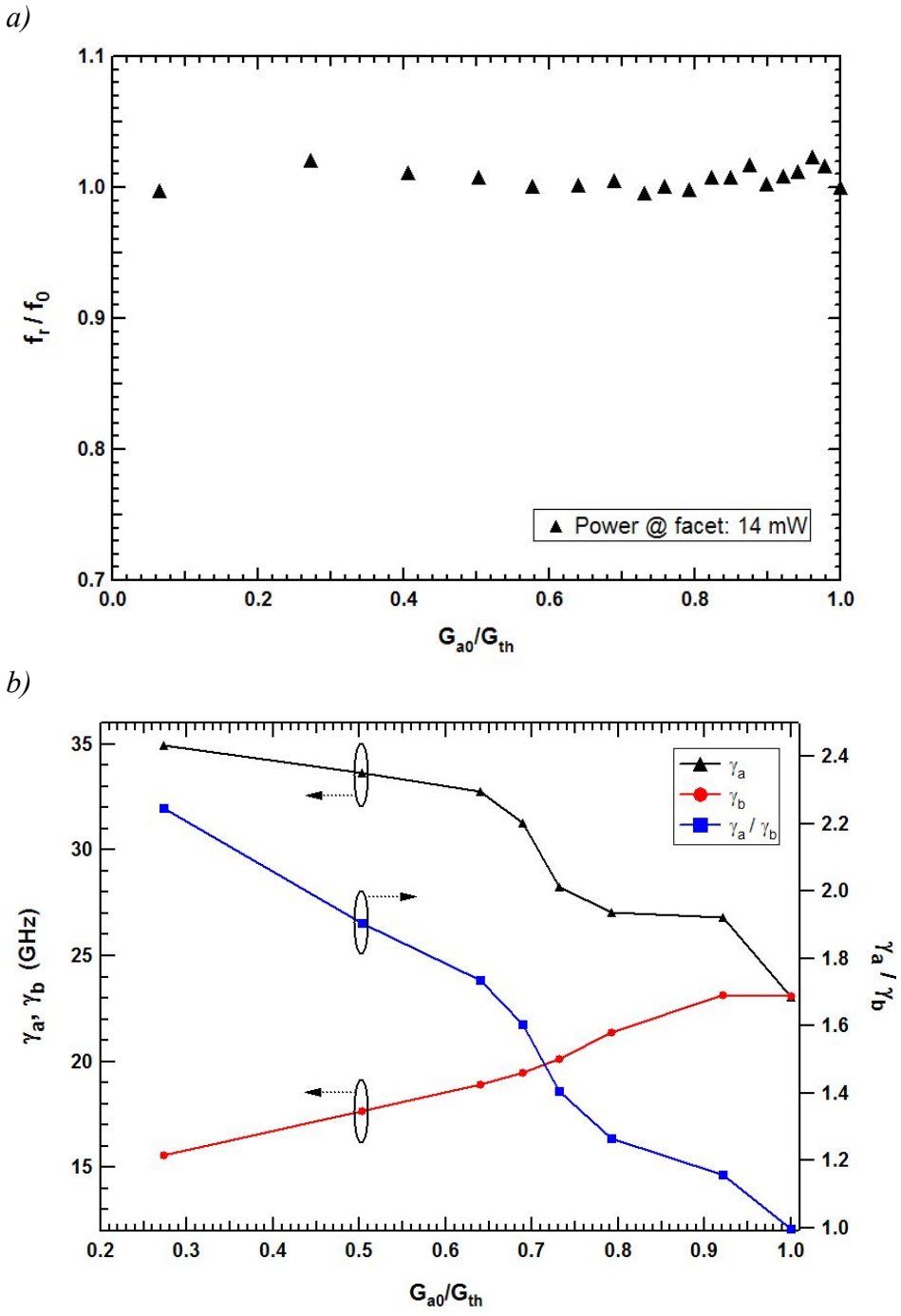

Figure (4.11) *a) Normalized resonance frequency as a function of normalized gain in the modulation section plotted based on the new two-section model, b) Extracted damping rates associated with the modulation and the gain sections as a function of normalized modulation section gain*

modulation efficiency enhancement of 8-dB. Note, however, that the maximum η was measured at $G_{a0}/G_{th} = 0.56$, not at $G_{a0}/G_{th} = 0.27$ where the gain-lever is a maximum. This is because of the interplay between the carrier lifetime and the stimulated lifetime. In terms of the damping rates, the two-section laser is operating in neither the purely photon density dominated regime nor the purely carrier lifetime dominated condition. It is somewhere between these extremes, but better described by two-section laser physics in any case. Finally, it is found that the current density applied to the modulation section cannot be too small so that G_{a0}/G_{th} must be greater than 0.25. Below $G_{a0}/G_{th} = 0.25$, the gain section would have to be pumped very hard in order to maintain the same output power to correspond with that of the uniform current level. This might shift the operation wavelength to that of the excited state of the QD and increase the non-linear effects that are undesirable.

4.4 Summary and Conclusion

The gain-lever effect is a useful tool to investigate and improve the modulation characteristics of semiconductor lasers, including mode-locked lasers. Previously this effect was studied in QWs and a modulation efficiency enhancement of 15 dB for amplitude modulation (in a 400 μm QW laser) and a 22 GHz/mA for frequency modulation was reported with no improvement in 3-dB bandwidth.

In this thesis, it is suggested that QD gain-levered devices are promising for high-speed modulation applications compared to QWs, due to the strong gain saturation effect in dots, and, consequently, the structure, performance and modulation characteristics of a two-section gain-lever QD laser are presented theoretically and experimentally. Based on this idea, an 8-dB enhancement in the modulation efficiency is demonstrated in a p-doped InAs/InGaAs QD gain-lever laser giving an approximate gain-lever value of 2.5. It was also discussed that under the high photon density approximation, the inverse carrier lifetime can be neglected in the damping rate. As a result, the damping rate ratio becomes the only reliable method for measuring the gain-lever since the modulation efficiency enhancement trends towards unity. Generally, higher modulation efficiency and thereby larger gain-lever values are expected in QD gain-lever devices due to higher differential gain ratio in these materials. But, it seems that the differential gain ratio (which is also proportional to the ratio of the damping rates) is limited by a short carrier lifetime and possibly stronger non-linear gain suppression in p-doped QD devices.

Also the validity of the single-section modulation response model was inspected.

We verified that this expression fails for a two-section configuration below a normalized modulation section gain value of 0.4 and that separate damping factors for each section need to be included in this instance.

The normalized 3-dB bandwidth as a function of gain in the modulation section for different power levels was also explored. It is found that the bandwidth becomes more power dependent with increased asymmetry in the two-section pumping or alternatively, lower threshold gain. Since at higher powers the probability of non-linear effects, such as non-linear gain suppression increases significantly, decreasing normalized bandwidth at higher powers and large pumping asymmetry may be also due to the non-linear gain suppression effect.

Using the small signal analysis and under a high photon density approximation, a new relative modulation response function for the two-section laser diode was derived in which two different damping rates are included to provide the damping and resonance frequency behavior in the device. According to the new derivation, this model has three poles in the denominator instead of the usual two associated with a single-section form and fits better with measured two-section responses rather than the single section model. Using the new response model, variation of the resonance frequency as a function of asymmetrical pumping is accurately modeled. In this model, for typical modulation section gain values with increased asymmetry in the two-section pumping, the gain and differential gain products in two sections are found to be nearly identical due to the parabolic shape of QD gain characteristics. As a result, the resonance frequency f_r,

remains almost the same for different pumping ratios with the same output power.

For future work it is desired to investigate the gain-lever effect for optimized QD device structures. For instance, modifying the waveguide structure can reduce the non-linear gain saturation effect to some extent which results in an improvement in the gain-lever effect. Theoretically, further improvement in the modulation efficiency enhancement and bandwidth can be achieved by using a shorter cavity length. Recently, there has been much research conducted to improve the 3-dB bandwidth of quantum dot lasers such as using p-doped QDs or lowering the temperature [4, 5, 8]. It is predicted that by using the gain-lever effect, higher AM and FM efficiency as well as about 50% improvement in 3-dB modulation bandwidth is possible in QD lasers.

Recently an optical injection locking technique has been combined with gain-lever modulation in DBR lasers to improve the radio frequency modulation performance. A 10-dB enhancement in the AM modulation efficiency and 3x increase in the modulation bandwidth is demonstrated [11]. This method can be also considered as a novel technique to improve the modulation performance of gain-lever semiconductor lasers for future efforts.

4.5 Chapter 4 References

[1] K. Y. Lau, "Broad wavelength tunability in gain-levered QW semiconductor laser," *Appl. Phys. Lett.,* 57, 2632 (1990)

[2] H. Olesen, et al., "Proposal of Novel Gain-Levered MQW DFB Lasers with High and Red-Shifted FM Response," *IEEE Photon. Technol. Lett,.* 5, 599 (1993)

[3] W. M. Yee, et al., "Enhanced Wavelength Tunability in Asymmetric Gain-Levered QW Semiconductor Laser," *J. Lightwave Technol.,* 13, 588 (1995)

[4] P. Bhattacharya, D. Klotzkin, O. Qasaimeh, W. Zhou, S. Krishna,and D. Zhu, "High-speed modulation and switching characteristics of In(Ga)As–Al(Ga)As self-organized quantum-dot lasers," *IEEE J. Select. Topics Quantum Electron.*, 6, 426–438, (2000)

[5] D. G. Deppe, et al., "Modulation Characteristics of QD Lasers: The Influence of P-Type Doping and the Electronic Density of States on Obtaining High Speed," *IEEE J. Quantum Electron*., 38, 1587 (2002);

[6] Y.–C. Xin, University of New Mexico, ECE Dep. Masters Thesis, (2003)

[7] N. Moore and K. Y. Lau, "Ultrahigh efficiency microwave signal transmission using tandem-contact single QW GaAlAs lasers," *Appl. Phys. Lett*., 55, 936 (1989)

[8] K. Y. Lau, "The Inverted Gain-Levered Semiconductor Laser-Direct Modulation with Enhanced Frequency Modulation and Suppressed Intensity Modulation," *IEEE Photon. Technol. Lett., 3, 703* (1990)

[9] H. Su and L. F. Lester, "Dynamic properties of QD distributed feedback lasers: high speed, linewidth and chirp," *J. Phys. D: Appl. Phys*., 38, 2112 (2005)

[10] N. A. Naderi, Y, Li and L. F. Lester, "Quantum dot gain-lever laser diode," *proceeding of IEEE/LEOS Annual Meeting,* Canada, (2006)

[11] Hyuk-Kee Sung, "Strong Optical Injection Locking of Edge-Emitting Lasers and Its Applications," UC Berkeley, EECS Dep. PHD dissertation, (2006)